Journal Pre-proof

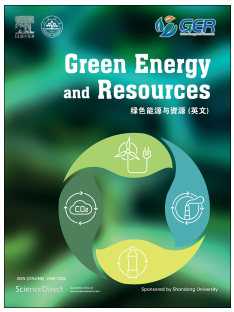

Biochar for heavy metal remediation in aquatic and terrestrial environments: Properties, influencing factors, and mechanisms

Yaoyao Cao, Jian Chen, Hui Zhang, Hongjie Sheng, Kang Lv, Jinjin Cheng, Xiaolong Chen, Dongfei Chen, Xiangyang Yu

PII: S2949-7205(26)00001-9

DOI: https://doi.org/10.1016/j.gerr.2026.100167

Reference: GER 100167

To appear in: *Green Energy and Resources*

Received Date: 3 September 2025

Revised Date: 10 December 2025

Accepted Date: 21 January 2026

Please cite this article as: Cao, Y., Chen, J., Zhang, H., Sheng, H., Lv, K., Cheng, J., Chen, X., Chen, D., Yu, X., Biochar for heavy metal remediation in aquatic and terrestrial environments: Properties, influencing factors, and mechanisms, *Green Energy and Resources*, https://doi.org/10.1016/j.gerr.2026.100167.

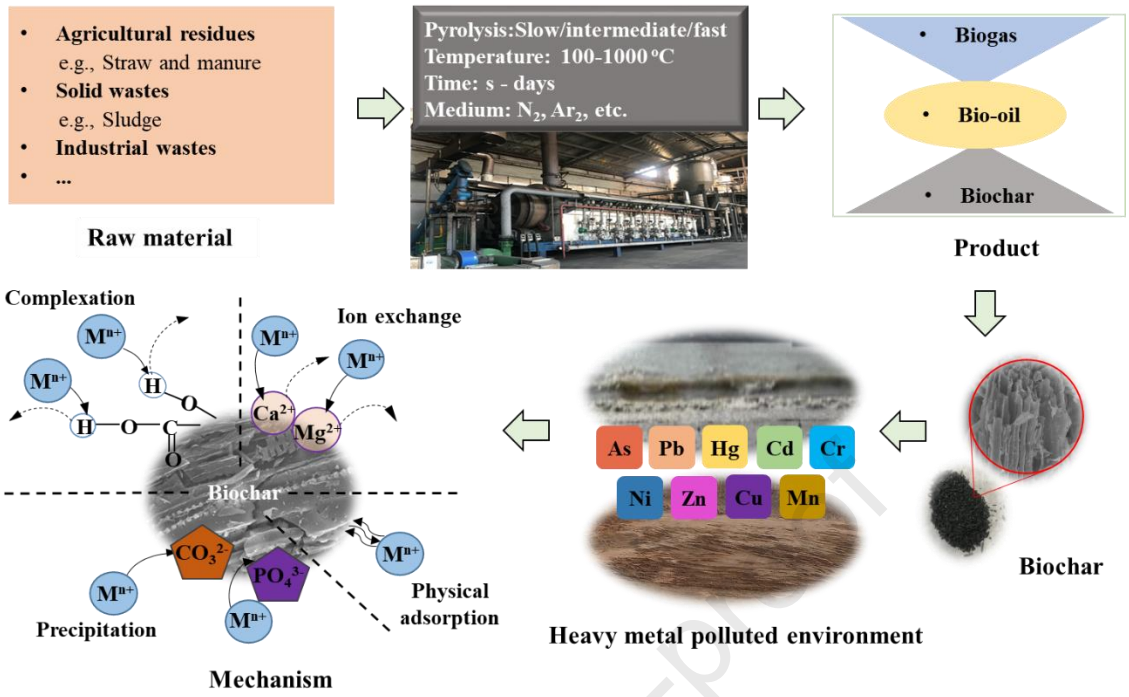

Graphical Abstract

Biochar for heavy metal remediation in aquatic and terrestrial environments: Properties, influencing factors, and mechanisms

Yaoyao Cao [a,b,c], Jian Chen [a,b,c], Hui Zhang [a,b,c], Hongjie Sheng [a,b,c], Kang Lv [a,b,c], Jinjin Cheng [a,b,c], Xiaolong Chen [a,b,c], Dongfei Chen [d], Xiangyang Yu [a,b,c*]

[a] *Jiangsu Key Laboratory for Food Quality and Safety-State Key Laboratory Cultivation Base, Ministry of Science and Technology, Nanjing 210014, China*

[b] *Key Laboratory of Control Technology and Standard for Agro-product Safety and Quality, Ministry of Agriculture and Rural Affairs, Nanjing 210014, China*

[c] *Institute of Food Safety and Nutrition, Jiangsu Academy of Agricultural Sciences, Nanjing 210014, China*

[d] *Graduate School of Biomedical Engineering, The University of New South Wales, Sydney, NSW 2052, Australia*

* Corresponding author. Fax/Tel: +86-25-84390396. E-mail address: yuxy@jaas.ac.cn (X. Yu)

Abstract: With the rapid development of industrialization, heavy metal pollution in water and soil has become increasingly serious. Biochar has attracted extensive attention for its application in heavy metal remediation, which mainly depends on its developed porous structure, large specific surface area, abundant functional groups and minerals. This review outline the status of heavy metal pollution and summarize the key physicochemical characteristics of biochar. Subsequently, a detailed analysis was conducted on the critical influencing factors, encompassing biochar physicochemical properties, environmental parameters, and heavy metal attributes. The core section comprehensively examines the primary remediation mechanisms, such as physical adsorption, ion exchange, precipitation, and complexation, highlighting how their relative importance shifts with biochar type and environmental context. Furthermore, remediation performance is not governed by a single mechanism but by the synergistic interplay of biochar's evolving surface chemistry, solution conditions, and metal speciation. Additionally, differences in dominant mechanisms and long-term stability are critically compared between aquatic and soil systems. Finally, we identify current knowledge gaps—particularly concerning short-term field performance, long-term aging effects, and sustainability under real-world conditions—and propose targeted future research directions to advance the practical, scalable, and safe application of biochar in heavy metal remediation.

Keywords: Heavy metal; Biochar; Physicochemical property; Influence factor; Remediation mechanism

1. Introduction

In recent years, the pollution of heavy metal in water and soil has become increasingly serious with the rapid development of industrialization, which is mainly caused by mining, smelting, fertilizers, and sewage irrigation (Ahmad et al., 2018; He et al., 2019; Khan et al., 2022; Li et al., 2017; Lin et al., 2025; Meng et al., 2018). According to the bulletin of soil contamination in China jointly issued by the Ministry of Environmental Protection and the Ministry of Land and Resources, the percentages of soil pollution sites exceeded 16.1%, and heavy metal was the main contaminant type, its pollution sites exceeded 82.8% (He et al., 2019; O'Connor et al., 2018; Tan et al., 2020; Wang et al., 2020). Also, heavy metal threatens human health through contaminated food chains, leading to serious problems such as brain damage, and kidney diseases, etc. (Fig.1). Therefore, it is a matter of people's health, environmental protection, and ecological safety to strengthen the prevention and control of heavy metal pollution in water and soil.

Heavy metal refers to the metal with a specific gravity greater than five, and molecular weight between 63.5 and 200.6, mainly including Arsenic (As), lead (Pb), mercury (Hg), cadmium (Cd), chromium (Cr), etc. (Chakma et al., 2025; Fu and Wang, 2011; Khan et al., 2022; Srivastava and Majumder, 2008). The top heavy metals and their maximum allowable contaminant level are shown in Table 1. Heavy metals enter aquatic and terrestrial systems through industrial effluents, mining and smelting activities, agricultural inputs (fertilizers and pesticides), atmospheric deposition and geological weathering. These pathways contribute to their widespread distribution and long-term ecological risks. The heavy metals contained in the water and soil are difficult to degrade, and easy to accumulate, which pose a serious threat to human health and the environment (Aghababaei et al., 2017; Fu and Wang, 2011; Tepanosyan et al., 2018;

63 Wang and Chen, 2009).

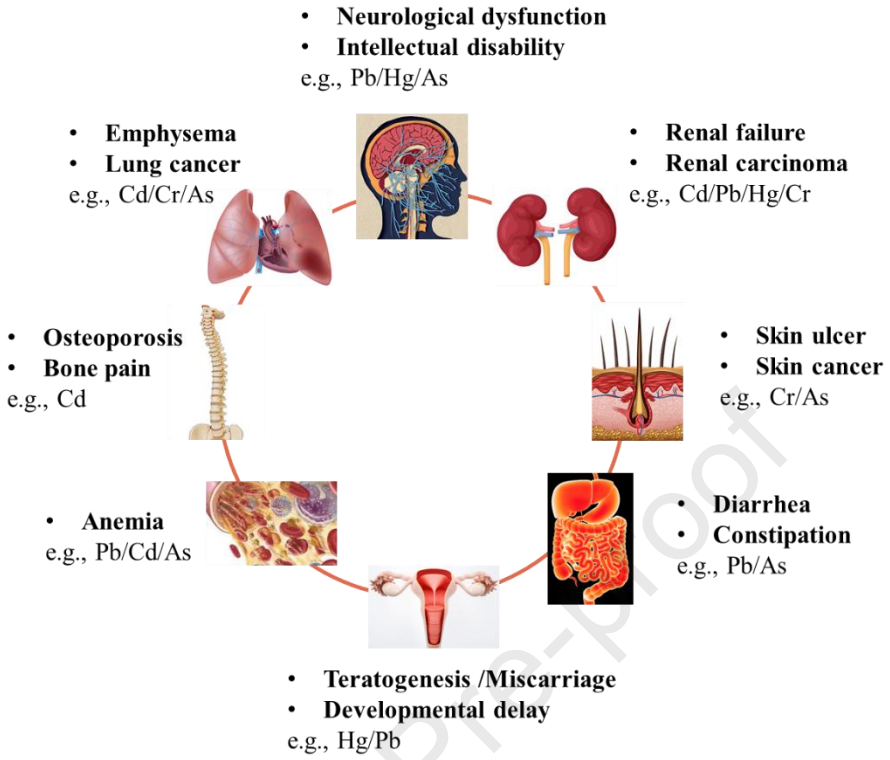

64

65 **Fig. 1** Human health risks from exposure to heavy metals.

66 **Table 1** Top heavy metals and their maximum allowable contaminant level (Inyang et

67 al., 2016; Srivastava and Majumder, 2008).

Heavy metals	Rank No. (CERCLA)	Maximum contaminant level by EPA (mg/L)
As	1	0.01
Pb	2	0.015
Hg	3	0.002
Cd	7	0.005
Cr	17	0.1

68 Note: CERCLA, Comprehensive Environmental Response Compensation and Liability

69 Act; EPA, Environmental Protection Agency.

70 The conventional heavy metal remediation technologies include chemical

71 precipitation, ion exchange, electrochemical and membrane separation for wastewater

(Aghababaei et al., 2017; Cui et al., 2016; Li et al., 2017; Li et al., 2023), and soil replacement, heat treatment, electrodynamic repair, chemical leaching, and plant repair for polluted soil (Kunkel et al., 2006; Robinson et al., 2003; Tognotti et al., 1991; Wasay et al., 2001). The methods have the advantages such as good removal effects, easy to recover heavy metals and disadvantages such as high cost, secondary pollution, etc. (shown in Table 2). Notably, the biosorption is the technology utilizing biological materials to removal the heavy metals, of which biochar is considered effective approach for the remediation of heavy metal in water and soil because of its low cost, simple methodology and environmentally friendly (Cui et al., 2016; He et al., 2019; Li et al., 2017; Wang et al., 2015; Wang et al., 2018). Despite extensive literature, a unified mechanistic framework linking biochar structure, environmental factors and metal species across different environments is still lacking. This review was prepared by systematically searching Web of Science, and Google Scholar for articles published up to September 2025. Search terms included combinations of “biochar”, “heavy metal”, “adsorption”, “remediation”, “influence”, and “mechanism”. Key studies were cross-checked in cited references to ensure comprehensive coverage. This review integrates the mechanisms of biochar–metal interactions across aquatic and terrestrial environments and emphasizes how feedstock, pyrolysis conditions, environmental factors and aging jointly determine remediation performance. Recent advances and future research needs are critically discussed to provide a systematic and forward-looking framework.

94 **Table 2** Technology for heavy metal remediation.

Matrix	Technology	Advantage	Disadvantage
Water	Chemical precipitation	Convenient, low cost, wide applicability	Sediment generated, difficult to handle
	Ion exchange	Materials can be reusable, high selectivity	High cost, low removal efficiency
	Electrochemical	Less chemical reagents, high selectivity and purity	High cost, strong current
	Membrane separation	Less solid waste and reagent, high removal efficiency	High cost, slow speed
Soil	Soil replacement	Efficiency	High cost, contaminated soil needs treatment
	Heat treatment	Efficiency	High cost
	Electrodynamic repair	Efficiency	High cost
	Chemical leaching	Long-lasting, simple operation	Secondary pollution
	Plant repair	Low cost, no secondary pollution	Long cycle, harsh conditions, slow effect

95 **2. Biochar**

96 Biochar, one carbon-rich product with highly aromatic and chemically stable, is
97 derived by thermal degradation of biomass under anaerobic or anoxic conditions
98 (Kambo and Dutta, 2015; Li and Li, 2023; Mimmo et al., 2014; Zhao et al., 2025). The
99 history of biochar can be traced back to more than 2,500 years ago, the Native
100 Americans of the Amazon basin improved the barren soil by adding a special fertilizer,
101 and this Indian soil "Terra Preta" mainly contained a large amount of incompletely
102 burned charcoal that was the so-called biochar (Laird et al., 2009; Lehmann et al., 2011;

Manyà, 2012). Besides, Lehmann pointed out that biochar could effectively reduce the greenhouse effect of carbon dioxide and showed the considerable economic value (Lehmann, 2007). Researches showed that the application of biochar was not only reflected in the improvement of soil physicochemical properties, but also can be used to repair pollution of heavy metals (Kan et al., 2016; Laird et al., 2009; Li et al., 2023; Meyer et al., 2011; Zhu et al., 2017).

Biochar can be produced by pyrolysis of various feedstocks, including agricultural residues (Cui et al., 2016; Jiang et al., 2012; Lin et al., 2025; Xu et al., 2023), industrial wastes (Shen et al., 2018; Srivastava and Majumder, 2008), and solid wastes (Bogusz and Oleszczuk, 2018; Chen et al., 2015; Li et al., 2022; Lu et al., 2012), and it is widely applied in areas such as heavy metal contamination remediation, energy production, and carbon sequestration and emissions reduction, etc. (shown in Fig.2). Pyrolysis, the preparation technology of biochar, involves complex chemical reactions containing the process that organic matter is continuously thermally decomposed to form gas-phase and solid-phase (i.e. biochar) (Kan et al., 2016). With the temperature of the reaction chamber decreasing, the compounds with higher polarity and molecular weight in the gas phase are liquefied into bio-oil, and the compounds with lower molecular weight are retained in syngas (Kan et al., 2016; Venderbosch and Prins, 2010). According to the heating rate, pyrolysis can be divided into slow, medium and fast pyrolysis (Ahmad et al., 2014; Manyà, 2012; Qambrani et al., 2017). The pyrolysis under different control conditions and their products are shown in Table 3.

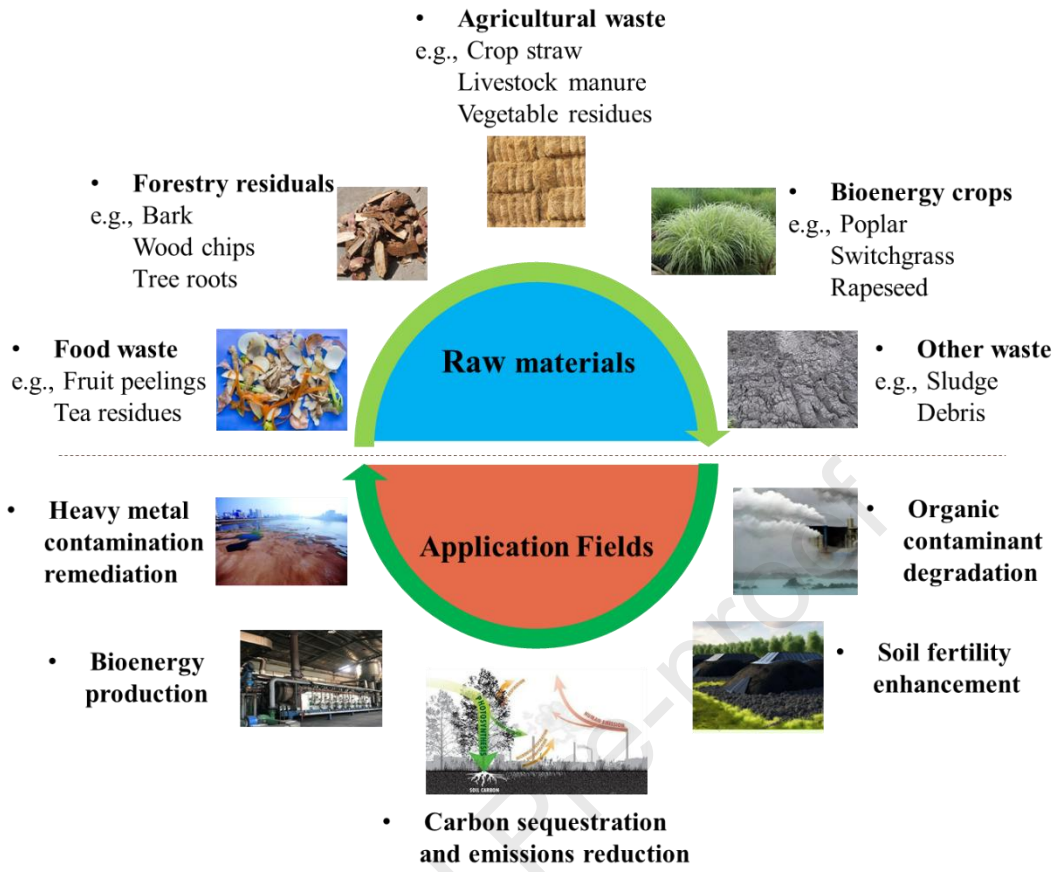

Fig. 2 Various sources and diverse applications of biochar.

Table 3 Typical products under different pyrolysis control conditions (Ahmad et al., 2014; Manyà, 2012; Qambrani et al., 2017; Zhang et al., 2019).

Classification	Pyrolysis temperature (°C)	Residence time	Production (%)		
			Solid	Gas	Liquid
Slow pyrolysis	100-1000	hour-days	35	35	30
Intermediate pyrolysis	~500	10-20 s	25	25	50
Fast pyrolysis	300-1000	< 2 s	12	13	75

The biochar mainly exhibits high carbon content, developed specific surface area and porosity, alkaline pH, strong ion exchange capacity, rich functional groups and high thermal stability (Feng et al., 2022; Kong et al., 2014; Novotny et al., 2015). Its physicochemical properties not only depend on the parameters of preparation (pyrolysis

132 temperature, residence time, and heating rate, etc.), but also on the composition and
133 structural characteristics of biomass raw materials (type, particle size, and pretreatment
134 methods, etc.) (Akhtar and Amin, 2012; Jaffari et al., 2023; Kan et al., 2016; Manyà,
135 2012), which are described as follows:

136 *2.1 Elemental composition*

137 Biochar contains the main elements of its raw material, while the differences exists
138 in the productions under the different pyrolysis processes (Ahmed et al., 2016; Jaffari
139 et al., 2023; Qambrani et al., 2017). The C in biochar is mainly derived from the
140 degradation of carbon-containing organic substances (Ahmad et al., 2014; Kan et al.,
141 2016). The content of H or O decreases with increasing pyrolysis temperature, mainly
142 due to the decomposition of organic matter to form volatile gases (such as carbon
143 dioxide, and nitrogen oxides) (Zhang et al., 2020). The content of N is relatively low,
144 Si is mostly enriched in the form of silicon oxide crystals, and Metal elements (such as
145 Na, Mg, K, and Ca) often exist in the form of chloride, carbonate, phosphate, and sulfate
146 (Kan et al., 2016; Wang et al., 2016). In terms of feedstock, wood-based biochars led
147 to greater C content over other biochars, while manures-based biochars contained the
148 greatest N, S, P, Ca, and Mg (Ippolito et al., 2020).

149 *2.2 Specific surface area*

150 Biochar has a well-developed pore structure and a large specific surface area
151 (SSA), which is mainly due to the continuous degradation of organic matter during
152 pyrolysis (Chen et al., 2025; Novotny et al., 2015; Rio et al., 2005). With the increasing
153 pyrolysis temperature, the degradation of organic matter is violent, which is beneficial
154 to the formation of pores and the exposure of surface area. However, the SSA decreases
155 at excessively high temperature, leading to destruction of the pore structure (clogging

or collapse, etc.) (Clough et al., 2013; Li et al., 2017; Ma et al., 2025). In addition, the differences in SSA exist between the different sources of biochar (Li et al., 2017; Tang et al., 2013; Xie et al., 2016).

2.3 pH

The pH of biochar is alkaline, and pH value increases with increasing pyrolysis temperature (Li et al., 2017; Suliman et al., 2016; Zhang et al., 2020). There is a significant correlation between the pH value and ash content, which is mainly due to the large amount of Na, Mg, K, Ca and carbonate generated during the preparation of biochar. Meanwhile, the functional groups on the surface (such as -COOH and -OH) are also one of the main reasons for its alkalinity (Li et al., 2017; Singh et al., 2010; Yan et al., 2024; Zhao et al., 2015).

2.4 Cation exchange capacity

The cation exchange capacity (CEC) refers to the exchange capacity between the cations in the biochar and the heavy metals in the water and soil, which can be influenced by the minerals in biochar (Han et al., 2020; Xu et al., 2017; Zhao et al., 2015). During the pyrolysis preparation of biochar, the CEC enhances as the metal minerals enriched. The CEC of biochar mainly depends on the content and type of its mineral components (Carrier et al., 2013; Leng et al., 2025; Uras et al., 2012), and has a certain correlation with the soluble cation content (Xu et al., 2017). Generally, the ash in crop straw is higher than that of wood, which is accordance with the fact that their CEC values (Huijgen et al., 2014).

2.5 Functional group

Biochar contains a wide variety of functional groups, including oxygen-containing functional groups (carboxyl, hydroxyl, ketone, and ester, etc.), and other active

functional groups (C=C and N-H with coordinated electron pairs, etc.) (Li et al., 2023; Qambrani et al., 2017; Uchimiya et al., 2011; Várhegyi et al., 1998). With the increasing pyrolysis temperature, the content of oxygen-containing functional groups decreases, while the aromatic ring compounds and carbon skeleton structures are generated, which is consistent with the decreasing atomic ratios of H/C, and O/C (Ahmed et al., 2016; Mukherjee et al., 2011; Zhao et al.). This phenomenon is mainly due to the formation of bio-oil by cellulose and hemicellulose, while lignin is retained as a carbon-based solid during the pyrolysis process (Akhtar and Amin, 2012; Yang et al., 2007).

3. Factors affecting biochar utilization for heavy metal remediation

Biochar shows great potential in the remediation of heavy metal polluted water and soil, because of its alkaline pH, strong ion exchange capacity, abundant functional group and minerals, etc. (Ahmad et al., 2014; Kong et al., 2014; Li et al., 2022; Shahzad et al., 2024; Yang et al., 2025). The biochar utilization for heavy metal remediation in water and soil is summarized in Table 4.

There are many factors affecting the remediation of heavy metal by biochar (Inyang et al., 2016; Shang and Chi, 2024; Uchimiya, 2014). Firstly, the removal efficiencies of heavy metals are different between biochars derived from different raw materials (Inyang et al., 2016; Xu et al., 2018). The composition, structure and pyrolysis conditions of raw materials directly affect the removal efficiencies of heavy metals (Uchimiya et al., 2011; Xiao et al., 2017; Xu et al., 2018). Furthermore, environmental factors (pH, ionic strength, organic matter content, and redox potential, etc.) and heavy metal properties (content, occurrence form, chemical valence state, etc.) will also have a certain impact on the removal efficiencies of heavy metals (Uchimiya et al., 2011; Uchimiya, 2014; Xiao et al., 2017; Xu et al., 2020; Xu and Zhao, 2013).

204 **Table 4** Biochar utilization for the remediation of heavy metal in water and soil.

Matrix	Feedstock/pyrolysis temperature (°C)	Heavy metal	Condition			Efficiency (mg/g)	Reference
			Dosage (g/L)	pH	Time (h)		
Water	Date palm/700	Cd(II)	2	5.0	24	43.58	(Usman et al., 2016)
	Date palm/300	Cd(II)	2	5.0	24	26.96	(Usman et al., 2016)
	Empty fruit bunch/600	Cd(II)	5	6.0	24	85	(Sadegh-Zadeh et al., 2017)
	Rice husk/600	Cd(II)	5	6.0	24	36	(Sadegh-Zadeh et al., 2017)
	Water hyacinth/450	Cd(II)	5	-	24	70.3	(Zhang et al., 2015)
	Corncob/550	Cd(II)	1	6.8	24	31.29	(Luo et al., 2018)
	Pine wood/400	Pb(II)	10	5.0	24	4.13	(Mohan et al., 2007)
	Wheat straw/600	Pb(II)	1	5.0	48	99.45	(Cao et al., 2019)
	Dairy manure/200	Pb(II)	5	-	4	109.4	(Cao et al., 2009)
	Alternanthera philoxeroides/600	Pb(II)	2	5.0	24	257.12	(Yang et al., 2014)
	Corn stalk/450	Pb(II)	2	5.5	24	49.7	(Liu et al., 2019)
	Tetra Pak/600	As(III)	2	-	24	24.2	(Ding et al., 2018)
	Tetra Pak/600	As(V)	2	-	24	33.2	(Ding et al.,

						2018)
Japanese oak wood/500	As(III)	1	7.0	2	3.16	(Niazi et al., 2018)
Japanese oak wood/500	As(V)	1	7.0	2	3.89	(Niazi et al., 2018)
Paper mill sludge/720	As(V)	1	-	24	22.8	(Yoon et al., 2017)
Banana peduncle/300	Cr(VI)	2	2.0	24	114	(Karim et al., 2015)
Wheat straw/500	Cr(VI)	2	3.0	24	12.23	(Zhu et al., 2016)
Sewage sludge/900	Cr(VI)	2	3.0	12	< 7	(Chen et al., 2015)
Sewage sludge/900	Cr(III)	2	3.0	12	25.27	(Chen et al., 2015)
Sewage sludge/300	Cr(VI)	12	-	3	64.10	(Agrafioti et al., 2014)
Sewage sludge/300	Cr(III)	12	-	3	94.34	(Agrafioti et al., 2014)
Sugarcane bagasse/600	Ni(II)	12	6.0	48	1949	(Lyu et al., 2018)
Opuntia ficus-indica cactus/600	Ni(II)	0.6	6.0	48	44	(Choudhary et al., 2020)
Dairy manure/350	Cu(II)	6	-	10	54.4	(Xu et al., 2013)
Opuntia ficus-indica cactus/600	Cu(II)	0.6	6.0	48	49	(Choudhary et al., 2020)
Rice straw/550	Zn(II)	1.25	5.0	48	39.46	(Zhao et al., 2020)
Dairy manure/350	Zn(II)	6	-	10	32.8	(Xu et al., 2013)

205

206 **Table 4** Biochar utilization for heavy metal remediation in water and soil. (*continued*)

Matrix	Feedstock/pyrolysis temperature (°c)	Heavy metals	Condition			Efficiency	Reference
			Dosage	pH	Time		
Soil	Wheat straw/350-550	Cd	10–40 t/hm^2	5.36	3 y	$CaCl_2$ extractable Cd was decreased by 54.5%–70.9%, 53.5%–64.8%, and 28.3%–60.9%.	(Bian et al., 2014)
	Wheat straw/350-550	Cd	20–40	5.01	2 y	$CaCl_2$ extractable Cd was significantly decreased by 39%–92%.	(Bian et al., 2013)
	Green waste/550	Cd	5%	-	14 d	NH_4NO_3 extractable Cd concentrations was reduced from 0.95 mg/kg to 0.67 mg/kg.	(Park et al., 2011)
	Chicken manure/550	Cd	5%	-	14 d	NH_4NO_3 extractable Cd concentrations was reduced from 0.95 mg/kg to 0.11 mg/kg.	(Park et al., 2011)
	Sugarcane bagasse/450	Cd	1.5–3 t/hm^2	5.8	30 d	Exchangeable Cd decreased from 8.5% (0.12 mg/kg) to 5.8% (0.08 mg/kg), 2.9% (0.04 mg/kg) and 2.9% (0.04 mg/kg).	(Nie et al., 2018)
	Wood/550	Cd	5–15 g/kg	6.38	10 w	The phosphate-extractable Cd was reduced from 0.28 mg/kg to 0.36 mg/kg, and 0.42 mg/kg.	(Namgay et al., 2010)

Water hyacinth/450	Cd	2%–5%	7.15	1 m	$CaCl_2$ extractable Cd was decreased from 1.31 mg/kg to 0.35 mg/kg, and 0.31 mg/kg.	(Yin et al., 2016)
Rice straw/450	Cd	2%–5%	7.15	1 m	$CaCl_2$ extractable Cd was decreased from 1.31 mg/kg to 0.81 mg/kg, and 0.49 mg/kg.	(Yin et al., 2016)
Wheat straw/450	Cd	10–40 t/hm^2	6.07	5 y	Exchangeable fractions of Cd were significantly decreased by 11.4%–44.6%, 19.8%–22.1%, 17.7%–22.1%, and 15.5%–24.2%.	(Cui et al., 2016)
Wheat straw/350-550	Pb	10–40 t/hm^2	5.36	3 y	$CaCl_2$ extractable Pb was reduced by 16.7%–33.3%, 65.0%–79.6%, and 18.1%–59.1%.	(Bian et al., 2014)
Green waste/550	Pb	5%	-	14 d	NH_4NO_3 extractable Pb concentrations was reduced from 11.3 mg/kg to 7.17 mg/kg.	(Park et al., 2011)
Chicken manure/550	Pb	5%	-	14 d	NH_4NO_3 extractable Pb concentrations was reduced from 11.3 mg/kg to 0.73 mg/kg.	(Park et al., 2011)
Sugarcane bagasse/450	Pb	1.5–3 t/hm^2	5.8	30 d	Exchangeable and carbonate bound fractions decreased from 21.0% (73.5 mg/kg) to 15.7% (54.9 mg/kg), 14.1% (48.7 mg/kg) and 12.6% (43.9 mg/kg).	(Nie et al., 2018)

Wheat straw/450	Pb	10–40 t/hm^2	6.07	5 y	Exchangeable fractions of Pb were significantly decreased by 14.2%–19.8%, 22.7%–45.5%, 40.8%–44.7%, and 28.2%–41.3%.	(Cui et al., 2016)
Water hyacinth/450	Pb	2%–5%	7.15	1 m	$CaCl_2$ extractable Pb was decreased from 2.81 mg/kg to 0.75 mg/kg, and 0.83 mg/kg.	(Yin et al., 2016)
Rice straw/450	Pb	2%–5%	7.15	1 m	$CaCl_2$ extractable Pb was decreased from 2.81 mg/kg to 1.59 mg/kg, and 1.09 mg/kg.	(Yin et al., 2016)
Water hyacinth/450	As	2%–5%	7.15	1 m	KH_2PO_4 extractable As was increased from 11.20 mg/kg to 11.97 mg/kg, and 12.52 mg/kg.	(Yin et al., 2016)
Rice straw/450	As	2%–5%	7.15	1 m	KH_2PO_4 extractable As was increased from 11.20 mg/kg to 11.92 mg/kg, and 13.07 mg/kg.	(Yin et al., 2016)
Wood/550	As	5–15 g/kg	6.38	10 w	The phosphate-extractable As was increased from 0.12 mg/kg to 0.24 mg/kg, and 0.22 mg/kg.	(Namgay et al., 2010)
Pine woodchip/450	As	3%	6.8	14 d	No significant difference in ammonium sulphate-extractable As between control and amended soil.	(Brennan et al., 2014)
Olive tree pruning/450	As	3%	6.8	14 d	Ammonium sulphate-extractable As was increased by 2 folds.	(Brennan et al., 2014)

Willow/350 & 550	As	10–20 g/kg	5.6	6 m	Compared to control soil, the concentration of water-soluble As had increased to the same value, the total As was increased by 14,000 mg/ha.	(Gregory et al., 2014)
Sugarcane bagasse/500	Cr	15 g/kg	7.54	4 m	Availability of Cr in the soil was reduced by 85%.	(Bashir et al., 2018)
Sugarcane bagasse/550	Cr	3%–7%	7.3	15 d	Bioavailable concentration of Cr was reduced from 23 mg/kg to 17.3 mg/kg, and 12.4 mg/kg.	(Khan et al., 2020)
Poplar wood/550	Cr	3%–7%	7.3	15 d	Bioavailable concentration of Cr was reduced from 23 mg/kg to 22.6 mg/kg, and 19.2 mg/kg.	(Khan et al., 2020)
Bagasse/600	Cr	2–10 g/kg	7.54	15 d	Immobilisation efficiency of Cr(VI) and Cr_{total} was 100% and 91.94%, respectively.	(Su et al., 2016)
Handwood/600	Ni	0.5%–2%	7.9	3 y	Residue fractions of Ni was increased from 51% to 61%–66%.	(Shen et al., 2016)
Willow/700	Ni	2.5%–10%	6.53	18 m	Ni content in fractions (exchangeable, water soluble and bound to carbonates) decreased by 57–75%.	(Bogusz and Oleszczuk, 2018)
Green waste/550	Cu	5%	-	14 d	NH_4NO_3 extractable Cu concentrations was reduced	(Park et al.,

					from 0.55 mg/kg to 0.42 mg/kg.	2011)
Sugarcane bagasse/450	Cu	1.5–3 t/hm^2	5.8	30 d	Two labile fractions (exchangeable and carbonate bound) decreased from 12.1% (33.9 mg/kg) to 8.7%, 6.3% and 6.1% (24.1, 17.4 and 16.9 mg/kg).	(Nie et al., 2018)
Handwood/600	Zn	0.5%–2%	7.9	3 y	Residue fractions of Zn was increased from 7% to 27%–35%.	(Shen et al., 2016)
Rice straw/500	Zn	0.75–22.5 t/hm^2	5.5	1 y	$CaCl_2$-extractable Zn concentrations were significantly decreased by 25.0%–83.6% for the paddy soil and 46.1%–90.3% for the wheat soil.	(Wu et al., 2018)
Holmoakwood/650	Zn	2%–4%	6.3	3 y	Acid-soluble fraction of Zn was reduced from 68%–81% to 65%–74%.	(Egene et al., 2018)

Note: y, year; m, month; w, week; d, day.

3.1 Effect of physicochemical properties of biochar on heavy metal remediation

As a pollution remediation agent, biochar's physicochemical properties (preparation method, type of raw materials, pyrolysis temperature, cation exchange capacity and surface charge, etc.) directly affect the removal efficiency of heavy metals (Inyang et al., 2016; Qi et al., 2024; Qian et al., 2016; Uchimiya et al., 2011; Xiao et al., 2023). Biochar preparation strongly influences its physicochemical properties and metal remediation capacity. Pyrolysis temperature, heating rate, residence time and reaction atmosphere determine aromaticity, surface area, porosity, functional groups, mineral phases and pH (Mandal et al., 2021). For instance, increasing pyrolysis temperature enhances aromatic structure and alkalinity but may reduce oxygen-containing groups that are crucial for complexation with metal cations (Manyà, 2012; Xiao et al., 202).

Usman et al. (2016) investigated the removal efficiency of Cd(II) onto different date palm-derived biochars (BC-300 and BC-700) under pyrolysis temperatures of 300 and 700 ºC, respectively, and found that the maximum adsorption capacity of 43.58 mg/g was observed for BC-700 based on the Langmuir model, which was 1.6 times higher than that of BC-300 (26.96 mg/g), indicating that pyrolysis temperature was the main factor determining the adsorption efficiency of different biochars. Uchimiya et al. (2011) studied the adsorption amounts of Pb, Cd, Ni, and Cd onto different cottonseed hull-based biochars (CH200, CH350, CH500, CH650, and CH800) under 200, 350, 500, 650, and 800 ºC for 4 h, respectively. The results suggested that CH350 was the most effective in removing heavy metals, the phenomenon was due to the strong electrostatic interactions between the negatively charged surfaces of biochar and heavy metal ions. Jiang et al. (2013) prepared different biochars (derived from maize straw, rice straw, and bagasse, respectively) at 400 ºC for 4 h to remove As in the polluted soil. Compared with the raw

materials, the adsorption amounts of As onto biochars increased significantly, especially the maize straw and rice straw-derived biochars, which were attributed to their larger cation exchange capacity.

The biochars derived from different raw material have different removal efficiency of different heavy metals, and the composition, structure and pyrolysis conditions of the raw materials directly determine the properties of biochar, thus affecting the removal efficiency of heavy metal (Park et al., 2011; Sadegh-Zadeh et al., 2017; Usman et al., 2016; Ye et al., 2025; Yin et al., 2016). Generally, the adsorption amount of heavy metals increases with the dosage increases to a certain extent and then reached equilibrium as the dosage continues to increase, mainly because the adsorption sites provided for the heavy metals are relatively saturated (Cao et al., 2019; Chen et al., 2015). In addition, the aging phenomenon of biochar is mainly manifested in the oxidation of adding oxygen-containing functional groups (such as carboxyl and hydroxyl groups, etc.), which causes an increase in negative charge, enhanced CEC, and improves/affects the removal efficiency of heavy metal (Kumar et al., 2018; Rechberger et al., 2019; Zhao et al., 2015).

3.2 Effect of environmental factors on heavy metal remediation

Environmental factors (pH, ionic strength, etc.) have varying degrees of influence on the adsorption of heavy metals onto biochar (Feng et al., 2022; Uchimiya, 2014; Xiao et al., 2023). Luo et al. (2018) investigated the removal efficiencies of Cd(II) in the different type soils by rape straw and peanut shell-derived biochars. The results showed that the Cd(II) removal efficiencies enhanced rapidly with the pH value increased from 2 to 4 and stabilized at pH 5–7, which was related to the fact that an increased pH decreases the competitiveness of Cd(II) against protons for binding sites, and the precipitation, hydroxide complexes of Cd(II) formed. Xu et al. (2020) studied the effects of $FeCl_3$ and

organic acids on remediation efficiency of Cr(VI) onto biochar, and found that $FeCl_3$ reduced the reduction rate of Cr(VI), mainly due to the covering effect between the iron mineral salts and the iron-biochar composite and the oxidation of biochar by Fe(III); while $FeCl_3$ and organic acid biochar can enhance the reduction rate of Cr(VI), the main reason is that Fe(III) was reducted to Fe(II) by organic acid, which accelerated electron transfer. Qian et al. (2019) analyzed the effects of ions on the remediation efficiency of Zn(II) and Cd(II) onto wheat straw-derived biochar, the results showed that the ions in the acidic environment weakens the remediation efficiency of heavy metals; while the ions in the alkaline environment can enhance the remediation efficiency of heavy metals.

As an important environmental factor, pH directly affects the existence speciation of heavy metal ions and the surface charge of biochar, thereby changing the way of attraction/repulsion between biochar and heavy metals (Tan et al., 2020; Uchimiya, 2014; Wang et al., 2018; Xiao et al., 2017; Yan et al., 2024). When the pH value is too low, there are more H^+ in the environment to form a strong competition with heavy metal ions, reducing its adsorption capacity (Luo et al., 2019; Xiao et al., 2017). Under fluctuating redox or pH conditions, dissolution of metal–biochar complexes or mineral phases may occur. Acidic conditions enhance proton competition, whereas reducing conditions can destabilize Fe/Mn oxide-bound metals, potentially causing desorption. Thus, long-term stability should be evaluated under cyclic redox environments (Luo et al., 2025; Wu, et al., 2025). On the other hand, ionic strength affects the amount of heavy metal onto biochar, which is mainly attribute to the coexisting ions occupying the active sites on the surface of the biochar and forming corresponding competition for heavy metals (Qian et al., 2019; Zhang et al., 2017). Furthermore, temperature mainly affects the thermodynamic process and adsorption heat capacity of biochar to adsorb heavy metals.

Generally, increasing the ambient temperature is beneficial to increase the amount of heavy metal onto biochar, mainly because the adsorption process is an endothermic reaction (Inyang et al., 2016; Luo et al., 2019; Xiao et al., 2017).

3.3 Effect of heavy metal properties on heavy metal remediation

The remediation efficiency of heavy metal is influenced by its properties (type of heavy metal, ionic radius, and charge, etc.) (Li et al., 2023; Qian et al., 2016; Xiao et al., 2023). Ko et al. (2004) investigated the ability of bone biochar to adsorb Cu(II), Zn(II) and Cd(II), and the selectivity of metal ions follows the order Cu(II) > Zn(II) > Cd(II), the reversed order of hydrated ionic radii is Cu(II) (4.19 Å) < Cd(II) (4.26 Å) < Zn(II) (4.30 Å). This result agrees with other studies (Lee and Moon, 2001; Wan Ngah and Hanafiah, 2008). Beesley et al. (2011) employed the difference of As, Cd, and Zn from a multi-element contaminated sediment-derived soil by a column leaching experiment, the results showed that the capability of biochar to immobilize Cd and Zn assisted a 300- and 45-fold reduction in their leachate concentrations, respectively. While the As concentration in eluate was not significantly reduced or increased during the leaching test, which was due to the fact that As was so weakly water-soluble in this soil. Zhao et al. (2020) indicated that the biochars had greater adsorption capacities for Pb(II) than for Zn(II), which was due to the former's higher electronegativity, lower pK_H (negative log of hydrolysis constant), and lower binding energy.

In the adsorption process, the competition between heavy metals is induced especially at high concentration, this is mainly attributable to differences in chemical characteristics between the heavy metals (Park et al., 2016). The enhanced remediation efficiency may be attributed to: (1) greater ionic radius (subsequently smaller hydrated radius), (2) higher hydrolysis constant, (3) higher atomic weight, and (4) larger

electronegativity, all of which provide the heavy metal with improved efficacy for inner sphere surface complexation or sorption reactions (Ko et al., 2004; Lee and Moon, 2001; Park et al., 2016; Wan Ngah and Hanafiah, 2008).

Overall, in aquatic environments, the adsorption capacities of biochars toward heavy metals vary substantially across feedstocks and pyrolysis temperatures (Usman et al., 2016; Sadegh-Zadeh et al., 2017). For instance, the Cd adsorption capacity of date-palm biochar increases from 26.96 mg g^{-1} at 300 °C to 43.58 mg g^{-1} at 700 °C (Usman et al., 2016), while Pb adsorption rises dramatically from 4.13 mg g^{-1} for pine-wood biochar pyrolyzed at 400 °C to 257.12 mg g^{-1} at 600 °C (Mohan et al., 2007; Yang et al., 2014). Likewise, Ni exhibits the highest overall sorption capacity among the evaluated metals, with high-temperature biochars achieving adsorption capacities exceeding 1900 mg g^{-1} (Lyu et al., 2018). These trends are primarily attributed to the enlarged specific surface area, increased mineral crystallinity, and enhanced aromaticity of biochars at elevated pyrolysis temperatures, which favor metal retention through mineral precipitation and surface complexation (Wang et al., 2024). However, the adsorption behaviors of anionic species such as As and Cr(VI) are more complex; their sorption efficiencies are generally lower and strongly influenced by solution pH (Chen et al., 2015; Ding et al., 2018; Niazi et al., 2018).

In soil systems, biochar functions predominantly by altering the speciation and distribution of heavy metals, thereby reducing their bioavailability and mobility (Nie et al., 2018; Khan et al., 2020). Numerous studies have shown that biochar application significantly decreases the exchangeable or weakly bound fractions of Cd, Pb, Cu, and Zn (e.g., $CaCl_2$-extractable or NH_4NO_3-extractable fractions). For example, wheat-straw biochars (350–550 °C) reduce $CaCl_2$-extractable Cd by 28.3–70.9% over a three-year

period (Bian et al., 2014). Similarly, poultry-manure biochar produced at 550 °C can markedly decrease NH_4NO_3-extractable Pb from 11.3 mg kg^{-1} to 0.73 mg kg^{-1} (Park et al., 2011). Notably, for As, some studies have reported increased or unchanged bioavailable concentrations following biochar addition, likely due to competitive interactions between arsenate/arsenite and phosphate-like functional groups on biochar surfaces, as well as elevated soil pH enhancing As solubility (Brennan et al., 2014; Yin et al., 2016).

Importantly, the mechanisms governing remediation differ fundamentally between aquatic and soil environments. In water, the process is dominated by rapid liquid–solid interfacial adsorption kinetics, controlled mainly by diffusion and the competition between H^+ and other cations (Park et al., 2016; Yoon et al., 2017). In contrast, soil remediation involves complex multiphase interfacial processes that integrate interactions among soil minerals, organic matter, plant roots, and microorganisms (Bashir et al., 2018; Xiao et al., 2023). Therefore, the remediation performance of biochar is not dictated by single variables such as pyrolysis temperature, metal speciation, or environmental pH, but rather by the interplay among pollutant chemical characteristics, biochar structural evolution during pyrolysis, and environmental application contexts (Suliman et al., 2016; Xiao et al., 2023; Zhao et al., 2015).

4. Main mechanism of heavy metal remediation by biochar

The physical properties of biochar, including pore structure, specific surface area, cation exchange capacity (CEC), and mineral content, directly influence adsorption and ion-exchange processes. Macropores facilitate metal diffusion, while micropores enhance surface interactions. CEC drives ion exchange between biochar-bound cations and target metals. Mineral components (e.g., carbonates, phosphates, Fe/Mn oxides) promote

precipitation or complexation. Environmental conditions such as pH and ionic strength modulate these pathways. It is essential to reveal the remediation mechanism for exploring the role of biochar in removing heavy metals in water and soil. According to the interaction forces between the adsorbent and adsorbate, the remediation mechanism can be divided into physical adsorption, ion exchange, precipitation and complexation (shown in Fig. 3) (Chakma et al., 2025; Demirbas, 2008; Inyang et al., 2016; Li et al., 2023; Robalds et al., 2016). As mentioned above, the differences exist between the feedstock, environment, and heavy metal, therefore the remediation mechanism is required and compared shown is Table 5.

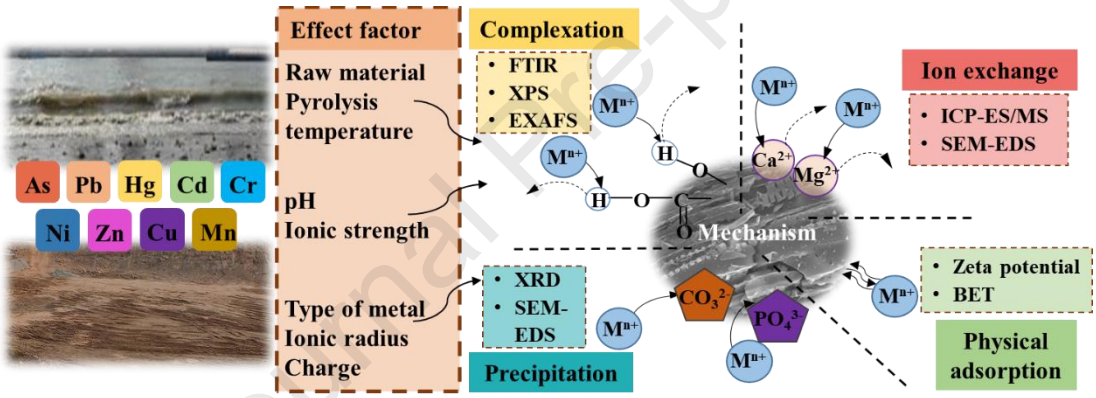

Fig. 3 The remediation mechanism of heavy metals by biochar (M, heavy metal).

Table 5 Mechanism of heavy metals remediation by biochar.

Matrix	Feedstock/pyrolysis temperature (°C)	Heavy metal	Main mechanism	Reference
Water	Date palm/700	Cd(II)	Precipitation	(Usman et al., 2016)
	Date palm/300	Cd(II)	Ion exchange, complexation	(Usman et al., 2016)
	Empty fruit bunch/600	Cd(II)	Complexation	(Sadegh-Zadeh et al.,

			2017)
Rice husk/600	Cd(II)	Complexation	(Sadegh-Zadeh et al., 2017)
Water hyacinth/450	Cd(II)	Ion exchange, complexation, precipitation	(Zhang et al., 2015)
Corncob/550	Cd(II)	Ion exchange, complexation	(Luo et al., 2018)
Pine wood/400	Pb(II)	Ion exchange	(Mohan et al., 2007)
Wheat straw/600	Pb(II)	Precipitation, cation exchange	(Cao et al., 2019)
Dairy manure/200	Pb(II)	Precipitation	(Cao et al., 2009)
Alternanthera philoxeroides/600	Pb(II)	Precipitation, complexation	(Yang et al., 2014)
Corn stalk/450	Pb(II)	Ion exchange, complexation, precipitation	(Liu et al., 2019)
Tetra Pak/600	As(III)	Complexation, precipitation	(Ding et al., 2018)
Tetra Pak/600	As(V)	Complexation	(Ding et al., 2018)
Japanese oak wood/500	As(III)	Complexation, precipitation, electrostatic interaction	(Niazi et al., 2018)
Japanese oak wood/500	As(V)	Complexation, precipitation, electrostatic interaction	(Niazi et al., 2018)
Banana peduncle/300	Cr(VI)	Reduction, complexation	(Karim et al., 2015)
Wheat straw/500	Cr(VI)	Electrostatic interaction, reduction	(Zhu et al., 2016)

	Sewage sludge/900	Cr(III)	Precipitation, cation exchange	(Chen et al., 2015)
	Sewage sludge/300	Cr(VI)	Electrostatic interaction, precipitation	(Agrafioti et al., 2014)
	Sewage sludge/300	Cr(III)	Electrostatic interaction, precipitation	(Agrafioti et al., 2014)
	Sugarcane bagasse/600	Ni(II)	Cation-π interaction, electrostatic interaction, complexation	(Lyu et al., 2018)
	Opuntia ficus-indica cactus/600	Ni(II)	Cation exchange, complexation, electrostatic interaction	(Choudhary et al., 2020)
	Dairy manure/350	Cu(II)	Precipitation, cation-π interaction, complexation	(Xu et al., 2013)
	Opuntia ficus-indica cactus/600	Cu(II)	Cation exchange, complexation, electrostatic interaction	(Choudhary et al., 2020)
	Rice straw/550	Zn(II)	Electrostatic interaction, cation exchange, complexation	(Zhao et al., 2020)
	Dairy manure/350	Zn(II)	Precipitation, cation-π interaction, complexation	(Xu et al., 2013)
Soil	Wheat straw/350-550	Cd	Precipitation, cation exchange, complexation	(Bian et al., 2014)
	Wheat straw/350-550	Cd	Precipitation	(Bian et al., 2013)
	Green waste/550	Cd	Precipitation, complexation	(Park et al., 2011)
	Chicken manure/550	Cd	Precipitation, complexation	(Park et al., 2011)
	Sugarcane bagasse/450	Cd	Complexation	(Nie et al., 2018)
	Wood/550	Cd	Complexation	(Namgay et al., 2010)

Water hyacinth/450	Cd	Complexation, precipitation, cation exchange	(Yin et al., 2016)
Rice straw/450	Cd	Complexation, precipitation, cation exchange	(Yin et al., 2016)
Wheat straw/450	Cd	Precipitation, complexation	(Cui et al., 2016)
Wheat straw/350-550	Pb	Precipitation, cation exchange, complexation	(Bian et al., 2014)
Green waste/550	Pb	Precipitation, complexation	(Park et al., 2011)
Chicken manure/550	Pb	Precipitation, complexation	(Park et al., 2011)
Sugarcane bagasse/450	Pb	Precipitation	(Nie et al., 2018)
Water hyacinth/450	Pb	Precipitation, complexation	(Yin et al., 2016)
Rice straw/450	Pb	Precipitation, complexation	(Yin et al., 2016)
Wheat straw/450	Pb	Precipitation, complexation	(Cui et al., 2016)
Wood/550	As	Complexation	(Namgay et al., 2010)
Water hyacinth/450	As	Complexation, precipitation	(Yin et al., 2016)
Rice straw/450	As	Complexation, precipitation	(Yin et al., 2016)
Willow/350 & 550	As	Precipitation	(Gregory et al., 2014)
Sugarcane bagasse/500	Cr	Precipitation	(Bashir et al., 2018)

Sugarcane bagasse/550	Cr	Precipitation	(Khan et al., 2020)
Poplar wood/550	Cr	Precipitation	(Khan et al., 2020)
Bagasse/600	Cr	Precipitation	(Su et al., 2016)
Handwood/600	Ni	Complexation, precipitation	(Shen et al., 2016)
Willow/700	Ni	Precipitation, electrostatic interaction, ion exchange, complexation	(Bogusz and Oleszczuk, 2018)
Green waste/550	Cu	Precipitation, complexation	(Park et al., 2011)
Sugarcane bagasse/450	Cu	Complexation	(Nie et al., 2018)
Handwood/600	Zn	Complexation, precipitation	(Shen et al., 2016)
Rice straw/500	Zn	Complexation, precipitation	(Wu et al., 2018)
Holmoakwood/650	Zn	Precipitation, complexation	(Egene et al., 2018)

4.1 Physical adsorption

The physical adsorption is electrostatic attraction or van der Waals force, and the adsorption is relatively weak (Rahim and Kassim, 2008; Xiao et al., 2025). Physical adsorption is mainly related to the specific surface area and porosity of the adsorbent (Elaigwu et al., 2014). Zeta potential analysis determines the surface charge of biochar under relevant pH conditions, clarifying its ability to attract or repel metal ions through electrostatic interactions (Choudhary et al., 2020). Brunauer–Emmett–Teller (BET)

371 analysis provides information on specific surface area, pore size distribution, and
372 structural morphology, demonstrating their positive correlation with heavy-metal uptake
373 and highlighting the contribution of physical adsorption. While Cao et al. (2018) found
374 the specific surface areas and pore volumes, were not vital parameters for determining
375 the adsorption capacity of Pb(II) onto wheat straw samples, the reason was that the
376 influence of physical adsorption on Pb(II) adsorption amount was negligible. Also, Hi
377 gashikawa et al. (2016) showed the removal efficiencies of Ni by sawdust-derived
378 biochars under 350 ºC (CM350) and 650 ºC (CM650) were 8.45 and 10.94 mg/g,
379 respectively, which may be due to the greater surface area and better development of the
380 microstructures at higher temperatures. Therefore, the increased specific surface area and
381 porosity could contribute to the adsorption of heavy metal when the physical adsorption
382 occupies a certain proportion in the adsorption mechanism.

383 *4.2 Ion exchange*

384 Ion exchange is mainly combined with the adsorbent through the exchange of cations
385 (Na^+, Mg^{2+}, K^+, and Ca^{2+}, etc.) and heavy metal ions (Ahmad et al., 2014; Ahmad et al.,
386 2018; Bian et al., 2014; Cao et al., 2018; Ma et al., 2025). Inductively coupled plasma
387 (ICP) analysis detects changes in solution-phase concentrations of alkali and alkaline
388 earth metal cations (K^+, Ca^{2+}, Mg^{2+}, Na^+) before and after adsorption, providing
389 quantitative evidence for cation exchange. Scanning electron microscopy coupled with
390 energy-dispersive X-ray spectroscopy (SEM–EDS) is employed to visualize the spatial
391 distribution of these exchangeable cations and their association with heavy metals at the
392 microscale (Niazi et al., 2018). Lu et al. (2012) studied the adsorption mechanism of Pb(II)
393 onto sludge-based biochar, the results showed that ion exchange accounted for the main
394 contribution (45.6% -60.2%), of which Ca^{2+} and Mg^{2+} play an important role instead of

395 K^+ and Na^+. While Wang and Liu (2017) investigated the capacities of biochars to remove
396 the heavy metals (Cu, Pb, Cd, and Zn), and K^+ played an important role in ion exchange
397 with heavy metals. Through ion exchange, heavy metal ions can form complexes with
398 organic functional groups (e.g. $-COO^-$, $-O^-$) by covalent bond (Bian et al., 2014; Liu et al.,
399 2019; Luo et al., 2018; Park et al., 2011; Usman et al., 2016).

400 *4.3 Precipitation*

401 Precipitation is the combination of heavy metal ions and anions (OH^-, CO_3^{2-}, PO_4^{3-},
402 SO_4^{2-}, and SiO_4^{4-}, etc.) in the adsorbent to form precipitated salts (Ahmad et al., 2014;
403 Ma et al., 2025; Wang et al., 2015; Xu et al., 2017). X-ray diffraction (XRD) reveals
404 newly formed crystalline mineral phases by identifying characteristic diffraction peaks
405 corresponding to heavy-metal precipitates (Cao et al., 2019). SEM–EDS complements
406 XRD by mapping microregions enriched in heavy metals and demonstrating their co-
407 localization with elements such as C and Ca, supporting the occurrence of mineral
408 precipitation (Cao et al., 2019). Zhang et al. (2017) analyzed removal efficiencies of Pb(II)
409 onto celery-derived biochars under 350 and 500 ºC, respectively. The results showed that
410 the precipitation contributed the most of adsorption mechanism, mainly in the form of
411 hydrocerussite ($2PbCO_3 \cdot Pb(OH)_2$) and hydro-pyromophite ($Pb_5(PO_4)_3OH$). Chen et al.
412 (2017) studied the precipitation mechanism of Pb onto wheat straw-derived biochar by
413 water-washing, and the contribution rate of anions (SO_4^{2-}, CO_3^{2-}, SiO_3^{2-} and PO_4^{3-})
414 followed the order: $SO_4^{2-} > CO_3^{2-} > SiO_3^{2-} > PO_4^{3-}$. Bian et al. (2014) pointed out that
415 precipitates ($Pb_5(PO_4)_3OH$ and $Cd(OH)_2$) were formed on the surface of biochar, which
416 was due to present of phosphate and hydroxide ions. Thus, the precipitation is directly
417 related to the cations or anions content, and is dominated by the mineral content (Cao et
418 al., 2019; Xu et al., 2017).

4.4 Complexation

Complexation mainly means the functional group on the surface of the adsorbent and heavy metal ions to share the electronic equivalent to form complexes (He et al., 2025; Wang et al., 2018; Zhang et al., 2017). Fourier-transform infrared spectroscopy (FTIR) verifies the participation of oxygen-containing functional groups—such as C=O and O–H—in metal coordination through characteristic peak shifts (Cao et al., 2019). X-ray photoelectron spectroscopy (XPS) provides electronic-level evidence by revealing changes in the O 1s high-resolution spectra (e.g., transformation of C=O to C–O–M structures) and the emergence or binding-energy shifts of metal-specific peaks (e.g., Pb 4f) (Xiao et al., 2025). Extended X-ray absorption fine structure (EXAFS) further confirms the formation of inner-sphere complexes by identifying atomic species (e.g., Pb–O), coordination numbers, and first-shell bond lengths (Lin et al., 2025). Uchimiya et al. (2011) revealed that the stabilization ability of heavy metals (especially Pb and Cu) by biochars directly correlated with their high containing oxygen functional groups, which could be investigated in detail by the method of Fourier-transform infrared spectroscopy (Song et al., 2014; Yuan et al., 2011). Yin et al. (2016) investigated that the varying effect of biochar on Cd, Pb and As mobility in a multi-metal contaminated paddy soil, the results revealed that the acidic functional groups and the hydroxylated surface of Fe/Mn oxides could contribute to Cd immobilization by providing more complexing sites. Wu et al. (2018) explored that the presence of biochar increased the proportion of Zn-organic material in soils, which was mainly due to the fact that organic material could form complexes with heavy metal, and surface oxygenated functional groups such as -OH and -COOH could provide the binding sites. The O, N, and S, etc. in the functional groups (-COOH, -OH, -NH, and –SH, etc.) can be used as coordinating atoms to provide electron

pair coordination with heavy metals (Qambrani et al., 2017; Rajapaksha et al., 2016).

The mechanistic evidence summarized in Table 5 supports the trends identified in Table 4 and further explains the variability observed across studies. At lower pyrolysis temperatures (<500 °C, particularly 300–450 °C), biochars retain abundant oxygen-containing functional groups (e.g., –COOH, –OH), relatively high cation exchange capacity (CEC), and a degree of amorphous carbon structure. Under these conditions, ion exchange and surface complexation serve as the dominant mechanisms governing the immobilization of cationic metals such as Cd and Cu (Choudhary et al., 2020; Usman et al., 2016; Yin et al., 2016). For example, Cd(II) adsorption by water-hyacinth biochar produced at 450 °C (70.3 mg g^{-1}) involves multiple mechanisms including ion exchange, complexation, and precipitation (Zhang et al., 2015).

In contrast, high-temperature biochars (>500 °C, especially ≥600 °C) exhibit markedly increased aromaticity, specific surface area, porosity, and surface alkalinity. These structural characteristics enhance precipitation, complexation, and physical adsorption interactions with heavy metals (Choudhary et al., 2020; Usman et al., 2016). For certain metals such as Ni and Cu, cation–π interactions also become significant, which refers to the electrostatic interaction between heavy metal cations and electron rich π clouds on aromatic rings in the graphitized region of biochar (Lyu et al., 2018). For instance, biochar produced from *Alternanthera philoxeroides* at 600 °C demonstrates a Pb(II) adsorption capacity of 257.12 mg g^{-1}, primarily driven by precipitation and complexation mechanisms (Yang et al., 2014). Notably, phosphorus-rich biochars (e.g., those derived from animal manure) tend to promote phosphate precipitation, whereas Ca/Mg-rich biochars (e.g., those produced from crop residues) facilitate carbonate precipitation (Cao et al., 2019; Xu et al., 2013).

Overall, cationic metals are mainly immobilized through ion exchange, electrostatic attraction, and mineral precipitation—processes favored by the high pH and mineral-rich surfaces produced at elevated pyrolysis temperatures (Yin et al., 2016; Bian et al., 2014). In contrast, oxyanion species rely predominantly on ligand exchange and surface complexation. These pathways diminish at higher temperatures as oxygen-containing functional groups volatilize (Gregory et al., 2014; Bashir et al., 2018; Khan et al., 2020). In summary, heavy-metal immobilization by biochar is governed by distinct dominant mechanisms in different environmental systems, yet ultimately results from the synergistic contributions of multiple interacting processes (Lin et al., 2025; Ma et al., 2025).

5. Challenge

Short-term adsorption performance of biochar in field environments is consistently lower than laboratory estimates. This discrepancy arises from competitive interactions with coexisting ions, the presence of natural organic matter, and temporally variable redox and pH conditions, which limit the effective availability of active sorption sites and reduce the metal-binding efficiency observed under idealized laboratory conditions (Lin et al., 2025; Ma et al., 2025).

Furthermore, Biochar exhibits declining regeneration efficiency during repeated adsorption–desorption cycles, this decrease is primarily associated with pore clogging, mineral precipitation, and the loss or transformation of surface functional groups (Guo et al., 2025; Chakma et al., 2025). Such structural and chemical degradation reduces the long-term stability of active sites and complicates efforts to maintain performance in dynamic environmental settings.

Biochar aging presents a major challenge to sustained heavy metal remediation

performance. Abiotic oxidation, biotic weathering, wet–dry and freeze–thaw cycles, and photo-oxidation collectively alter surface chemistry, pore architecture, and mineral composition (Kumar et al., 2018; Long et al., 2024). Although aging can increase oxygen-containing functional groups, enhancing complexation for some metals, it may also induce physical degradation, pore collapse, and blockage (Kumar et al., 2018; Ma et al., 2025). Therefore, aging effects are context-dependent; we recommend standardized aging tests and multi-cycle regeneration studies to assess long-term stability.

In addition, scaling up biochar applications faces significant constraints related to feedstock variability, technological bottlenecks, and economic constraints (Aziz, 2024). Additional concerns arise from the potential release of polycyclic aromatic hydrocarbons (PAHs), heavy metals, nanoparticles, and soluble organic fractions, particularly when biochar is derived from contaminated or inadequately pyrolyzed feedstocks, posing ecological risks, including adverse effects on soil biota and water quality (Guo et al., 2024; Long et al., 2024).

6. Conclusion and Prospects

This review synthesizes current knowledge on biochar properties, influencing factors and remediation mechanisms for heavy metals in aquatic and terrestrial environments. The key conclusions are as follows: (1) The remediation performance of biochar is highly dependent on feedstock type, pyrolysis parameters, and environment conditions; (2) Complexation, ion exchange and mineral precipitation often co-occur and their relative importance is system-specific; (3) Aging, redox/pH dynamics and natural organic matter critically modulate stability and must be systematically tested.

Overall, Biochar has a great potential for application in the heavy metal remediation. At present, the existing research has focused on the improvement of heavy metal

remediation, its influence factors and related mechanism, etc. However, the aging of biochar, its component release, and the effects of complex environment systems during heavy metal remediation are very limited. Considering the application of biochar, it is very important to evaluate its stability, repeatability and reproducibility (Awual et al., 2013; Aziz, 2024; Huang et al., 2017; Xu et al., 2018). The water-soluble components in biochar are rich in carboxylic acid, humic acid, soluble mineral ions, and nanoparticles, posing potential environmental risks, thus the relevant studies on pretreatment method is necessary to minimize the negative impacts (Feng et al., 2022; Ghidotti et al., 2017; Guo et al., 2024; Smith et al., 2016). At the same time, most of the experiments on heavy metal remediation by biochar are performed in laboratory, but there is still lack of data for natural conditions. Thus, the long-term monitoring research on heavy metal remediation by biochar in the water and soil needs to be improved.

Future development directions focus on: (1) Adopt standardized reporting (feedstock, pyrolysis conditions, full characterization, and experimental matrices); (2) Employ spectroscopic/microscopic methods to link mechanisms to evidence; (3) Implement standardized aging tests and multi-cycle regeneration studies to assess long-term stability; (4) Perform pilot field trials with safety evaluation (soluble organics, PAHs and heavy metal in nanoparticles) and life-cycle economic assessment before scale-up. These targeted steps will accelerate safe, effective deployment of biochar for heavy-metal remediation.

CRediT authorship contribution statement

Yaoyao Cao: Data curation, Funding acquisition, Visualization, Writing - original draft. **Jian Chen**: Formal analysis, Writing - review & editing. **Hui Zhang**: Methodology, Validation. **Hongjie Sheng**: Conceptualization, Investigation. **Kang Lv**: Methodology,

Validation. **Jinjin Cheng**: Formal analysis, Investigation. **Xiaolong Chen**: Formal analysis, Writing - review and editing. **Dongfei Chen**: Data curation, Writing - review and editing. **Xiangyang Yu**: Conceptualization, Funding acquisition, Supervision, Writing - review & editing.

Declaration of competing interest

The authors declare that they have no known competing financial interests or personal relationships that could have appeared to influence the work reported in this paper.

Acknowledgments

This study was funded by the National Natural Science Foundation of China (No. 32302406, and 32272600).

References

Aghababaei, A., Ncibi, M.C., Sillanpää, M., 2017. Optimized removal of oxytetracycline and cadmium from contaminated waters using chemically-activated and pyrolyzed biochars from forest and wood-processing residues. Bioresour. Technol. 239, 28-36. https://doi.org/10.1016/j.biortech.2017.04.119.

Agrafioti, E., Kalderis, D., Diamadopoulos, E., 2014. Arsenic and chromium removal from water using biochars derived from rice husk, organic solid wastes and sewage sludge. J. Environ. Manage. 133, 309-314. https://doi.org/10.1016/j.jenvman.2013.12.007.

Ahmad, M., Rajapaksha, A.U., Lim, J.E., Zhang, M., Bolan, N., Mohan, D., Vithanage, M., Lee, S.S., Ok, Y.S., 2014. Biochar as a sorbent for contaminant management in soil and water: a review. Chemosphere 99, 19-33.

https://doi.org/10.1016/j.chemosphere.2013.10.071.

Ahmad, Z., Gao, B., Mosa, A., Yu, H., Yin, X., Bashir, A., Ghoveisi, H., Wang, S., 2018. Removal of Cu(II), Cd(II) and Pb(II) ions from aqueous solutions by biochars derived from potassium-rich biomass. J. Clean. Prod. 180, 437-449. https://doi.org/10.1016/j.jclepro.2018.01.133.

Ahmed, M.B., Zhou, J.L., Ngo, H.H., Guo, W., 2016. Insight into biochar properties and its cost analysis. Biomass Bioenergy 84, 76-86. https://doi.org/10.1016/j.biombioe.2015.11.002.

Akhtar, J., Amin, N.S., 2012. A review on operating parameters for optimum liquid oil yield in biomass pyrolysis. Renew. Sust. Energ. Rev. 16 (7), 5101-5109. https://doi.org/10.1016/j.rser.2012.05.033.

Awual, M.R., Yaita, T., El-Safty, S.A., Shiwaku, H., Suzuki, S., Okamoto, Y., 2013. Copper(II) ions capturing from water using ligand modified a new type mesoporous adsorbent. Chem. Eng. J. 221, 322-330. https://doi.org/10.1016/j.cej.2013.02.016.

Aziz, K.H.H., 2024. Removal of toxic heavy metals from aquatic systems using low-cost and sustainable biochar: A review. Desalin. Water Treat. 320, 100757. https://doi.org/10.1016/j.dwt.2024.100757.

Bashir, S., Hussain, Q., Akmal, M., Riaz, M., Hu, H., Ijaz, S.S., Iqbal, M., Abro, S., Mehmood, S., Ahmad, M., 2018. Sugarcane bagasse-derived biochar reduces the cadmium and chromium bioavailability to mash bean and enhances the microbial activity in contaminated soil. J. Soils Sediments 18 (3), 874-886. https://doi.org/10.1007/s11368-017-1796-z.

Beesley, L., Marmiroli, M., 2011. The immobilisation and retention of soluble arsenic, cadmium and zinc by biochar. Environ. Pollut. 159 (2), 474-480.

https://doi.org/10.1016/j.envpol.2010.10.016.

Bian, R., Chen, D., Liu, X., Cui, L., Li, L., Pan, G., Xie, D., Zheng, J., Zhang, X., Zheng, J., Chang, A., 2013. Biochar soil amendment as a solution to prevent Cd-tainted rice from china: Results from a cross-site field experiment. Ecol. Eng. 58, 378-383. https://doi.org/10.1016/j.ecoleng.2013.07.031.

Bian, R., Joseph, S., Cui, L., Pan, G., Li, L., Liu, X., Zhang, A., Rutlidge, H., Wong, S., Chia, C., Marjo, C., Gong, B., Munroe, P., Donne, S., 2014. A three-year experiment confirms continuous immobilization of cadmium and lead in contaminated paddy field with biochar amendment. J. Hazard. Mater. 272, 121-128. https://doi.org/10.1016/j.jhazmat.2014.03.017.

Bogusz, A., Oleszczuk, P., 2018. Sequential extraction of nickel and zinc in sewage sludge- or biochar/sewage sludge-amended soil. Sci. Total Environ. 636, 927-935. https://doi.org/10.1016/j.scitotenv.2018.04.072.

Brennan, A., Jiménez, E.M., Puschenreiter, M., Alburquerque, J.A., Switzer, C., 2014. Effects of biochar amendment on root traits and contaminant availability of maize plants in a copper and arsenic impacted soil. Plant Soil 379 (1-2), 351-360. https://doi.org/10.1007/s11104-014-2074-0.

Cao, X., Ma, L., Gao, B., Harris, W., 2009. Dairy-manure derived biochar effectively sorbs lead and atrazine. Environ. Sci. Technol. 43 (9), 3285-3291. https://doi.org/10.1021/es803092k.

Cao, Y., Xiao, W., Shen, G., Ji, G., Zhang, Y., Gao, C., Han, L., 2019. Carbonization and ball milling on the enhancement of Pb(II) adsorption by wheat straw: Competitive effects of ion exchange and precipitation. Bioresour. Technol. 273, 70-76. https://doi.org/10.1016/j.biortech.2018.10.065.

Cao, Y., Xiao, W., Shen, G., Ji, G., Zhang, Y., Gao, C., Han, L.J., 2018. Mechanical fragmentation of wheat straw at different plant scales: Pb^{2+} adsorption behavior and mechanism. Bioresources 13 (3), 6613-6630. https://doi.org/10.15376/biores.13.3.6613-6630.

Carrier, M., Joubert, J., Danje, S., Hugo, T., Görgens, J., Knoetze, J.H., 2013. Impact of the lignocellulosic material on fast pyrolysis yields and product quality. Bioresour. Technol. 150, 129-138. https://doi.org/10.1016/j.biortech.2013.09.134.

Chakma, S., Hasan, M., Hu, Y., Rakshit, S.K., Kang, K., 2025. Valorization of red mud and biomass waste via pre-pyrolysis activation for high-performance magnetic biochar in heavy metal remediation. Waste Manage. 204, 114970. https://doi.org/10.1016/j.wasman.2025.114970.

Chen, C., Hu, Y., Ge, Y., Tao, J., Yan, B., Cheng, Z., Lv, X., Cui, X., Chen, G., 2025. Integrated learning framework for enhanced specific surface area, pore size, and pore volume prediction of biochar. Bioresour. Technol. 424, 132279. https://doi.org/10.1016/j.biortech.2025.132279.

Chen, D., Li, R., Bian, R., Li, L., Joseph, S., Crowley, D., Pan, G., 2017. Contribution of soluble minerals in biochar to Pb^{2+} adsorption in aqueous solutions. Bioresources 12 (1), 1662-1679. https://doi.org/10.15376/biores.12.1.1662-1679.

Chen, M., Wang, D., Yang, F., Xu, X., Xu, N., Cao, X., 2017. Transport and retention of biochar nanoparticles in a paddy soil under environmentally-relevant solution chemistry conditions. Environ. Pollut. 230, 540-549. https://doi.org/10.1016/j.envpol.2017.06.101.

Chen, T., Zhou, Z., Han, R., Meng, R., Wang, H., Lu, W., 2015. Adsorption of cadmium by biochar derived from municipal sewage sludge: Impact factors and adsorption

mechanism. Chemosphere 134, 286-293. https://doi.org/10.1016/j.chemosphere.2015.04.052.

Chen, T., Zhou, Z., Xu, S., Wang, H., Lu, W., 2015. Adsorption behavior comparison of trivalent and hexavalent chromium on biochar derived from municipal sludge. Bioresour. Technol. 190, 388-394. https://doi.org/10.1016/j.biortech.2015.04.115.

Choudhary, M., Kumar, R., Neogi, S., 2020. Activated biochar derived from *opuntia ficus-indica* for the efficient adsorption of malachite green dye, Cu^{+2} and Ni^{+2} from water. J. Hazard. Mater. 392, 122441. https://doi.org/10.1016/j.jhazmat.2020.122441.

Clough, T., Condron, L., Kammann, C., Müller, C., 2013. A review of biochar and soil nitrogen dynamics. Agronomy-Basel 3 (2), 275-293. https://doi.org/10.3390/agronomy3020275.

Cui, L., Pan, G., Li, L., Bian, R., Liu, X., Yan, J., Quan, G., Ding, C., Chen, T., Liu, Y., Liu, Y., Yin, C., Wei, C., Yang, Y., Hussain, Q., 2016. Continuous immobilization of cadmium and lead in biochar amended contaminated paddy soil: A five-year field experiment. Ecol. Eng. 93, 1-8. https://doi.org/10.1016/j.ecoleng.2016.05.007.

Cui, X., Fang, S., Yao, Y., Li, T., Ni, Q., Yang, X., He, Z., 2016. Potential mechanisms of cadmium removal from aqueous solution by *canna indica* derived biochar. Sci. Total Environ. 562, 517-525. https://doi.org/10.1016/j.scitotenv.2016.03.248.

Demirbas, A., 2008. Heavy metal adsorption onto agro-based waste materials: A review. J. Hazard. Mater. 157 (2-3), 220-229. https://doi.org/10.1016/j.jhazmat.2008.01.024.

Ding, Z., Xu, X., Phan, T., Hu, X., Nie, G., 2018. High adsorption performance for As(III) and As(V) onto novel aluminum-enriched biochar derived from abandoned tetra paks. Chemosphere 208, 800-807. https://doi.org/10.1016/j.chemosphere.2018.06.050.

Egene, C.E., Van Poucke, R., Ok, Y.S., Meers, E., Tack, F.M.G., 2018. Impact of organic

amendments (biochar, compost and peat) on Cd and Zn mobility and solubility in contaminated soil of the Campine region after three years. Sci. Total Environ. 626, 195-202. https://doi.org/10.1016/j.scitotenv.2018.01.054.

Elaigwu, S.E., Rocher, V., Kyriakou, G., Greenway, G.M., 2014. Removal of pb^{2+} and cd^{2+} from aqueous solution using chars from pyrolysis and microwave-assisted hydrothermal carbonization of *prosopis africana* shell. J. Ind. Eng. Chem. 20 (5), 3467-3473. https://doi.org/10.1016/j.jiec.2013.12.036.

Feng, L., He, S., Zhao, W., Ding, J., Liu, J., Zhao, Q., Wei, L., 2022. Can biochar addition improve the sustainability of intermittent aerated constructed wetlands for treating wastewater containing heavy metals? Chem. Eng. J. 444, 136636. https://doi.org/10.1016/j.cej.2022.136636.

Fu, F., Wang, Q., 2011. Removal of heavy metal ions from wastewaters: A review. J. Environ. Manage. 92 (3), 407-418. https://doi.org/10.1016/j.jenvman.2010.11.011.

Ghidotti, M., Fabbri, D., Mašek, O., Mackay, C.L., Montalti, M., Hornung, A., 2017. Source and biological response of biochar organic compounds released into water; Relationships with bio-oil composition and carbonization degree. Environ. Sci. Technol. 51 (11), 6580-6589. https://doi.org/10.1021/acs.est.7b00520.

Gregory, S.J., Anderson, C.W.N., Camps Arbestain, M., McManus, M.T., 2014. Response of plant and soil microbes to biochar amendment of an arsenic-contaminated soil. Agr. Ecosyst. Environ. 191, 133-141. https://doi.org/10.1016/j.agee.2014.03.035.

Guo, P., Li, Z., Luo, J., Xu, X., Liu, H., Cao, Y., Wei, Y., Liu, Z., Qing, Y., Wu, Y., 2025. Synergistic Se/S functionalization of biochar for effective immobilization of multi-target heavy metals in water and soil. J. Hazard. Mater. 500, 140453.

https://doi.org/10.1016/j.jhazmat.2025.140453

Guo, W., Yao, X., Chen, Z., Liu, T., Wang, W., Zhang, S., Xian, J., Wang, Y., 2024. Recent advance on application of biochar in remediation of heavy metal contaminated soil: Emphasis on reaction factor, immobilization mechanism and functional modification. J. Environ. Manage. 371, 123212. https://doi.org/10.1016/j.jenvman.2024.123212.

Han, L., Sun, K., Yang, Y., Xia, X., Li, F., Yang, Z., Xing, B., 2020. Biochar's stability and effect on the content, composition and turnover of soil organic carbon. Geoderma 364, 114184. https://doi.org/10.1016/j.geoderma.2020.114184.

He, L., Zhong, H., Liu, G., Dai, Z., Brookes, P.C., Xu, J., 2019. Remediation of heavy metal contaminated soils by biochar: Mechanisms, potential risks and applications in china. Environ. Pollut. 252, 846-855. https://doi.org/10.1016/j.envpol.2019.05.151.

He, Y., Chen, L., Zhang, X., Deng, Q., Zhang, H., Mo, X., Huang, Y., Lv, X., Mi, B., Wu, F., 2025. Discrepancies in measurement methods for biochar’s heavy metal adsorption performance caused by its dissolved organic matters. J. Hazard. Mater. 495, 139081. https://doi.org/10.1016/j.jhazmat.2025.139081.

Higashikawa, F.S., Conz, R.F., Colzato, M., Cerri, C.E.P., Alleoni, L.R.F., 2016. Effects of feedstock type and slow pyrolysis temperature in the production of biochars on the removal of cadmium and nickel from water. J. Clean. Prod. 137, 965-972. https://doi.org/10.1016/j.jclepro.2016.07.205.

Huang, X., An, D., Song, J., Gao, W., Shen, Y., 2017. Persulfate/electrochemical/$FeCl_2$ system for the degradation of phenol adsorbed on granular activated carbon and adsorbent regeneration. J. Clean. Prod. 165, 637-644. https://doi.org/10.1016/j.jclepro.2017.07.171.

706 Huijgen, W.J.J., Telysheva, G., Arshanitsa, A., Gosselink, R.J.A., de Wild, P.J., 2014.
707 Characteristics of wheat straw lignins from ethanol-based organosolv treatment. Ind.
708 Crop. Prod. 59, 85-95. https://doi.org/10.1016/j.indcrop.2014.05.003.
709 Inyang, M.I., Gao, B., Yao, Y., Xue, Y., Zimmerman, A., Mosa, A., Pullammanappallil,
710 P., Ok, Y.S., Cao, X., 2016. A review of biochar as a low-cost adsorbent for aqueous
711 heavy metal removal. Crit. Rev. Environ. Sci. Technol. 46 (4), 406-433.
712 https://doi.org/10.1080/10643389.2015.1096880.
713 Ippolito, J.A., Cui, L., Kammann, C., Mönnig, N.W., Jose, M.E., Mendizabal, T.F.,
714 Cayuela, M.L., Sigua, G., Novak, J., Spokas, K., Borchard, N., 2020. Feedstock
715 choice, pyrolysis temperature and type infuence biochar characteristics: A
716 comprehensive meta-data analysis review. Biochar 2, 421-438.
717 https://doi.org/10.1007/s42773-020-00067-x.
718 Jaffari, Z.H., Abbas, A., Kim, C.M., Shin, J., Kwak, J., Son, C., Lee, Y.G., Kim, S., Chon,
719 K., Cho, K.H., 2023. Transformer-based deep learning models for adsorption capacity
720 prediction of heavy metal ions toward biochar-based adsorbents. J. Hazard. Mater.
721 462, 132773. https://doi.org/10.1016/j.jhazmat.2023.132773.
722 Jiang, J., Xu, R., Jiang, T., Li, Z., 2012. Immobilization of Cu(II), Pb(II) and Cd(II) by
723 the addition of rice straw derived biochar to a simulated polluted ultisol. J. Hazard.
724 Mater. 229-230, 145-150. https://doi.org/10.1016/j.jhazmat.2012.05.086.
725 Jiang, J.P., Yuan, X.B., Ye, L.L., Liao, S.C., Zhang, X.H., 2013. Characteristics of straw
726 biochar and its influence on the forms of arsenic in heavy metal polluted soil. Applied
727 Mechanics and Materials 409-410, 133-138.
728 https://doi.org/10.4028/www.scientific.net/AMM.409-410.133.
729 Kambo, H.S., Dutta, A., 2015. A comparative review of biochar and hydrochar in terms

730 of production, physico-chemical properties and applications. Renew. Sust. Energ. Rev.
731 45, 359-378. https://doi.org/10.1016/j.rser.2015.01.050.
732 Kan, T., Strezov, V., Evans, T.J., 2016. Lignocellulosic biomass pyrolysis: A review of
733 product properties and effects of pyrolysis parameters. Renew. Sust. Energ. Rev. 57,
734 1126-1140. https://doi.org/10.1016/j.rser.2015.12.185.
735 Karim, A.A., Kumar, M., Mohapatra, S., Panda, C.R., Singh, A., 2015. Banana peduncle
736 biochar: Characteristics and adsorption of hexavalent chromium from aqueous
737 solution. International Research Journal of Pure & Applied Chemistry 1 (7), 1-10.
738 https://doi.org/10.9734/irjpac/2015/16163.
739 Khan, A.Z., Khan, S., Ayaz, T., Brusseau, M.L., Khan, M.A., Nawab, J., Muhammad, S.,
740 2020. Popular wood and sugarcane bagasse biochars reduced uptake of chromium and
741 lead by lettuce from mine-contaminated soil. Environ. Pollut. 263, 114446.
742 https://doi.org/10.1016/j.envpol.2020.114446.
743 Khan, Z., Fan, X., Khan, M.N., Khan, M.A., Zhang, K., Fu, Y., Shen, H., 2022. The
744 toxicity of heavy metals and plant signaling facilitated by biochar application:
745 implications for stress mitigation and crop production. Chemosphere 308 (Pt 3),
746 136466. https://doi.org/10.1016/j.chemosphere.2022.136466.
747 Ko, D.C.K., Cheung, C.W., Choy, K.K.H., Porter, J.F., McKay, G., 2004. Sorption
748 equilibria of metal ions on bone char. Chemosphere 54 (3), 273-281.
749 https://doi.org/10.1016/j.chemosphere.2003.08.004.
750 Kong, L., Liu, W., Zhou, Q., 2014. Biochar: An effective amendment for remediating
751 contaminated soil, In: Whitacre, D. (Eds.) Reviews of Environmental Contamination
752 and Toxicology. Springer, New York, pp. 83-99. https://doi.org/10.1007/978-3-319-
753 01619-1_4.

754 Kumar, A., Joseph, S., Tsechansky, L., Privat, K., Schreiter, I.J., Schüth, C., Graber, E.R.,
755 2018. Biochar aging in contaminated soil promotes Zn immobilization due to changes
756 in biochar surface structural and chemical properties. Sci. Total Environ. 626, 953-
757 961. https://doi.org/10.1016/j.scitotenv.2018.01.157.
758 Kunkel, A.M., Seibert, J.J., Elliott, L.J., Kelley, R.L., Katz, L.E., Pope, G.A., 2006.
759 Remediation of elemental mercury using in situ thermal desorption (ISTD). Environ.
760 Sci. Technol. 40 (7), 2384-2389. https://doi.org/10.1021/es0503581.
761 Laird, D.A., Brown, R.C., Amonette, J.E., Lehmann, J., 2009. Review of the pyrolysis
762 platform for coproducing bio-oil and biochar. Biofuel. Bioprod. Bior. 3 (5), 547-562.
763 https://doi.org/10.1002/bbb.169.
764 Lee, D.H., Moon, H., 2001. Adsorption equilibrium of heavy metals on natural zeolites.
765 Korean J. Chem. Eng. 18 (2), 247-256. https://doi.org/10.1007/BF02698467.
766 Lehmann, J., 2007. A handful of carbon. Nature 447 (7141), 143-144.
767 https://doi.org/10.1038/447143a.
768 Lehmann, J., Rillig, M.C., Thies, J., Masiello, C.A., Hockaday, W.C., Crowley, D., 2011.
769 Biochar effects on soil biota – A review. Soil Biol. Biochem. 43 (9), 1812-1836.
770 https://doi.org/10.1016/j.soilbio.2011.04.022.
771 Leng, L., Zheng, H., Shen, T., Wu, Z., Xiong, T., Liu, S., Cao, J., Peng, H., Zhan, H., Li,
772 H., 2025. Engineering biochar from biomass pyrolysis for effective adsorption of
773 heavy metal: An innovative machine learning approach. Sep. Purif. Technol. 361,
774 131592. https://doi.org/10.1016/j.seppur.2025.131592.
775 Li, B., Li, K., 2023. Efficient removal of both heavy metal ion and dyes from wastewater
776 using magnetic response adsorbent of block polymer brush-grafted N-doped biochar.
777 Chemosphere 340, 139811. https://doi.org/10.1016/j.chemosphere.2023.139811.

Li, C., Li, J., Xie, S., Zhang, G., Pan, L., Wang, R., Wang, G., Pan, X., Wang, Y., Angelidaki, I., 2022. Enhancement of heavy metal immobilization in sewage sludge biochar by combining alkaline hydrothermal treatment and pyrolysis. J. Clean. Prod. 369, 133325. https://doi.org/10.1016/j.jclepro.2022.133325.

Li, H., Dong, X., Da Silva, E.B., de Oliveira, L.M., Chen, Y., Ma, L.Q., 2017. Mechanisms of metal sorption by biochars: Biochar characteristics and modifications. Chemosphere 178, 466-478. https://doi.org/10.1016/j.chemosphere.2017.03.072.

Li, Q., Yin, J., Wu, L., Li, S., Chen, L., 2023. Effects of biochar and zero valent iron on the bioavailability and potential toxicity of heavy metals in contaminated soil at the field scale. Sci. Total Environ. 897, 165386. https://doi.org/10.1016/j.scitotenv.2023.165386.

Li, S., Wen, Y., Wang, Y., Liu, M., Su, L., Peng, Z., Zhou, Z., Zhou, N., 2023. Novel alpha-amino acid-like structure decorated biochar for heavy metal remediation in acid soil. J. Hazard. Mater. 462, 132740. https://doi.org/10.1016/j.jhazmat.2023.132740.

Lin, H., Xie, J., Dong, Y., Liu, J., Meng, K., Jin, Q., 2025. A complete review on the surface functional groups in pyrolyzed biochar and its interaction mechanism with heavy metal in water. J. Environ. Chem. Eng. 13 (3), 116681. https://doi.org/10.1016/j.jece.2025.116681.

Liu, L., Huang, Y., Zhang, S., Gong, Y., Su, Y., Cao, J., Hu, H., 2019. Adsorption characteristics and mechanism of Pb(II) by agricultural waste-derived biochars produced from a pilot-scale pyrolysis system. Waste Manage. 100, 287-295. https://doi.org/10.1016/j.wasman.2019.08.021.

Long, X., Yu, Z., Liu, S., Gao, T., Qiu, R., 2024. A systematic review of biochar aging and the potential eco-environmental risk in heavy metal contaminated soil. J. Hazard.

Mater. 472, 134345. https://doi.org/10.1016/j.jhazmat.2024.134345.

Lu, H., Zhang, W., Yang, Y., Huang, X., Wang, S., Qiu, R., 2012. Relative distribution of Pb^{2+} sorption mechanisms by sludge-derived biochar. Water Res. 46 (3), 854-862. https://doi.org/10.1016/j.watres.2011.11.058.

Luo, M., Lin, H., He, Y., Li, B., Dong, Y., Wang, L., 2019. Efficient simultaneous removal of cadmium and arsenic in aqueous solution by titanium-modified ultrasonic biochar. Bioresour. Technol. 284, 333-339. https://doi.org/10.1016/j.biortech.2019.03.108.

Luo, M., Lin, H., Li, B., Dong, Y., He, Y., Wang, L., 2018. A novel modification of lignin on corncob-based biochar to enhance removal of cadmium from water. Bioresour. Technol. 259, 312-318. https://doi.org/10.1016/j.biortech.2018.03.075.

Luo, J., Cai, Y., Yu, J., Huang, J., Yan, J., 2025. Phosphate-modified biochar- mineral-based composites for heavy metal removal in acidic environments: development and efficiency. Appl. Clay Sci. 276, 107924. https://doi.org/10.1016/j.clay.2025.107924.

Lyu, H., Gao, B., He, F., Zimmerman, A.R., Ding, C., Huang, H., Tang, J., 2018. Effects of ball milling on the physicochemical and sorptive properties of biochar: Experimental observations and governing mechanisms. Environ. Pollut. 233, 54-63. https://doi.org/10.1016/j.envpol.2017.10.037.

Ma, R., Luo, J., Duan, X., Sheng, Y., Wang, S., Zhang, D., Wang, F., Yang, S., Yi, W., 2025. Novel laser-driven fast pyrolysis of biomass: Insights into biochar characteristics and applications. Bioresour. Technol. 436, 132986. https://doi.org/10.1016/j.biortech.2025.132986.

Ma, Y., Zhang, F., Cheng, L., Zhang, D., Wu, X., Ma, Y., Liu, X., Xing, B., 2025. Remediation potential of biochar for as and cd by modifying soil physicochemical

properties: A conceptual model elucidating stabilization mechanism based on conditional probability theory. Biochar 7 (1), 63. https://doi.org/10.1007/s42773-025-00455-1.

Mandal, S., Pu, S., Adhikari, S., Ma, H., Kim, D., Bai, Y., Hou, D., 2021. Progress and future prospects in biochar composites: Application and reflection in the soil environment, Crit. Rev. Environ. Sci. Technol. 51(3), 219-271. https://doi.org/10.1080/10643389.2020.1713030

Manyà, J.J., 2012. Pyrolysis for biochar purposes: A review to establish current knowledge gaps and research needs. Environ. Sci. Technol. 46 (15), 7939-7954. https://doi.org/10.1021/es301029g.

Meng, J., Tao, M., Wang, L., Liu, X., Xu, J., 2018. Changes in heavy metal bioavailability and speciation from a Pb-Zn mining soil amended with biochars from co-pyrolysis of rice straw and swine manure. Sci. Total Environ. 633, 300-307. https://doi.org/10.1016/j.scitotenv.2018.03.199.

Meyer, S., Glaser, B., Quicker, P., 2011. Technical, economical, and climate-related aspects of biochar production technologies: A literature review. Environ. Sci. Technol. 45 (22), 9473-9483. https://doi.org/10.1021/es201792c.

Mimmo, T., Panzacchi, P., Baratieri, M., Davies, C.A., Tonon, G., 2014. Effect of pyrolysis temperature on miscanthus (*miscanthus* × *giganteus*) biochar physical, chemical and functional properties. Biomass Bioenergy 62, 149-157. https://doi.org/10.1016/j.biombioe.2014.01.004.

Mohan, D., Pittman, C.U., Bricka, M., Smith, F., Yancey, B., Mohammad, J., Steele, P.H., Alexandre-Franco, M.F., Gómez-Serrano, V., Gong, H., 2007. Sorption of arsenic, cadmium, and lead by chars produced from fast pyrolysis of wood and bark during

bio-oil production. J. Colloid. Interface. Sci. 310 (1), 57-73. https://doi.org/10.1016/j.jcis.2007.01.020.

Mukherjee, A., Zimmerman, A.R., Harris, W., 2011. Surface chemistry variations among a series of laboratory-produced biochars. Geoderma 163 (3-4), 247-255. https://doi.org/10.1016/j.geoderma.2011.04.021.

Namgay, T., Singh, B., Singh, B.P., 2010. Influence of biochar application to soil on the availability of As, Cd, Cu, Pb, and Zn to maize. Aust. J. Soil Res. 48 (6-7), 638. https://doi.org/10.1071/SR10049.

Niazi, N.K., Bibi, I., Shahid, M., Ok, Y.S., Shaheen, S.M., Rinklebe, J., Wang, H., Murtaza, B., Islam, E., Farrakh Nawaz, M., Lüttge, A., 2018. Arsenic removal by japanese oak wood biochar in aqueous solutions and well water: Investigating arsenic fate using integrated spectroscopic and microscopic techniques. Sci. Total Environ. 621, 1642-1651. https://doi.org/10.1016/j.scitotenv.2017.10.063.

Nie, C., Yang, X., Niazi, N.K., Xu, X., Wen, Y., Rinklebe, J., Ok, Y.S., Xu, S., Wang, H., 2018. Impact of sugarcane bagasse-derived biochar on heavy metal availability and microbial activity: A field study. Chemosphere 200, 274-282. https://doi.org/10.1016/j.chemosphere.2018.02.134.

Novotny, E.H., Maia, C.M.B.D., Carvalho, M.T.D.M., Madari, B.E., 2015. Biochar: pyrogenic carbon for agricultural use - A critical review. Rev. Bras. Cienc. Solo 39 (2), 321-344. https://doi.org/10.1590/01000683rbcs20140818.

O'Connor, D., Peng, T., Zhang, J., Tsang, D.C.W., Alessi, D.S., Shen, Z., Bolan, N.S., Hou, D., 2018. Biochar application for the remediation of heavy metal polluted land: A review of in situ field trials. Sci. Total Environ. 619-620, 815-826. https://doi.org/10.1016/j.scitotenv.2017.11.132.

874 Park, J., Ok, Y.S., Kim, S., Cho, J., Heo, J., Delaune, R.D., Seo, D., 2016. Competitive
875 adsorption of heavy metals onto sesame straw biochar in aqueous solutions.
876 Chemosphere 142, 77-83. https://doi.org/10.1016/j.chemosphere.2015.05.093.
877 Park, J.H., Choppala, G.K., Bolan, N.S., Chung, J.W., Chuasavathi, T., 2011. Biochar
878 reduces the bioavailability and phytotoxicity of heavy metals. Plant Soil 348 (1-2),
879 439-451. https://doi.org/10.1007/s11104-011-0948-y.
880 Qambrani, N.A., Rahman, M.M., Won, S., Shim, S., Ra, C., 2017. Biochar properties and
881 eco-friendly applications for climate change mitigation, waste management, and
882 wastewater treatment: A review. Renew. Sust. Energ. Rev. 79, 255-273.
883 https://doi.org/10.1016/j.rser.2017.05.057.
884 Qi, G., Pan, Z., Zhang, X., Wang, H., Chang, S., Wang, B., Gao, B., 2024. Novel
885 pretreatment with hydrogen peroxide enhanced microwave biochar for heavy metals
886 adsorption: Characterization and adsorption performance. Chemosphere 346, 140580.
887 https://doi.org/10.1016/j.chemosphere.2023.140580.
888 Qian, L., Zhang, W., Yan, J., Han, L., Gao, W., Liu, R., Chen, M., 2016. Effective
889 removal of heavy metal by biochar colloids under different pyrolysis temperatures.
890 Bioresour. Technol. 206, 217-224. https://doi.org/10.1016/j.biortech.2016.01.065.
891 Qian, T., Wu, P., Qin, Q., Huang, Y., Wang, Y., Zhou, D., 2019. Screening of wheat straw
892 biochars for the remediation of soils polluted with Zn (II) and Cd (II). J. Hazard. Mater.
893 362, 311-317. https://doi.org/10.1016/j.jhazmat.2018.09.034.
894 Rahim, A.A., Kassim, J., 2008. Recent development of vegetal tannins in corrosion
895 protection of iron and steel. Recent Patents on Materials Science 100 (3), 223-231.
896 https://doi.org/10.2174/1874465610801030223
897 Rajapaksha, A.U., Chen, S.S., Tsang, D.C.W., Zhang, M., Vithanage, M., Mandal, S.,

Gao, B., Bolan, N.S., Ok, Y.S., 2016. Engineered/designer biochar for contaminant removal/immobilization from soil and water: potential and implication of biochar modification. Chemosphere 148, 276-291. https://doi.org/10.1016/j.chemosphere.2016.01.043.

Rechberger, M.V., Kloss, S., Wang, S., Lehmann, J., Rennhofer, H., Ottner, F., Wriessnig, K., Daudin, G., Lichtenegger, H., Soja, G., Zehetner, F., 2019. Enhanced Cu and Cd sorption after soil aging of woodchip-derived biochar: What were the driving factors? Chemosphere 216, 463-471. https://doi.org/10.1016/j.chemosphere.2018.10.094.

Rio, S., Faur-Brasquet, C., Le Coq, L., Le Cloirec, P., 2005. Structure characterization and adsorption properties of pyrolyzed sewage sludge. Environ. Sci. Technol. 39 (11), 4249-4257. https://doi.org/10.1021/es0497532.

Robalds, A., Naja, G.M., Klavins, M., 2016. Highlighting inconsistencies regarding metal biosorption. J. Hazard. Mater. 304, 553-556. https://doi.org/10.1016/j.jhazmat.2015.10.042.

Robinson, B., Green, S., Mills, T., Clothier, B., Velde, M.V.D., Laplane, R., Fung, L., Deurer, M., Hurst, S., Thayalakumaran, T., Dijssel, C.V.D., 2003. Phytoremediation: Using plants as biopumps to improve degraded environments. Soil Res. 41 (3), 599. https://doi.org/10.1071/SR02131.

Sadegh-Zadeh, F., Samsuri, A.W., Seh-Bardan, B.J., Emadi, M., 2017. The effects of acidic functional groups and particle size of biochar on Cd adsorption from aqueous solutions. Desalin. Water Treat. 66, 309-319. https://doi.org/10.5004/dwt.2017.20216.

Shahzad, A., Zahra, A., Li, H.Y., Qin, M., Wu, H., Wen, M.Q., Ali, M., Iqbal, Y., Xie, S.H., Sattar, S., Zafar, S., 2024. Modern perspectives of heavy metals alleviation from oil contaminated soil: A review. Ecotoxicol. Environ. Saf. 282, 116698.

https://doi.org/10.1016/j.ecoenv.2024.116698.

Shang, Q., Chi, J., 2024. Mechanistic insight into the effects of interaction between biochar and soil with different properties on phenanthrene sorption. J. Environ. Manage. 367, 121961. https://doi.org/10.1016/j.jenvman.2024.121961.

Shen, Z., Som, A.M., Wang, F., Jin, F., McMillan, O., Al-Tabbaa, A., 2016. Long-term impact of biochar on the immobilisation of nickel (II) and zinc (II) and the revegetation of a contaminated site. Sci. Total Environ. 542, 771-776. https://doi.org/10.1016/j.scitotenv.2015.10.057.

Shen, Z., Tian, D., Zhang, X., Tang, L., Su, M., Zhang, L., Li, Z., Hu, S., Hou, D., 2018. Mechanisms of biochar assisted immobilization of Pb^{2+} by bioapatite in aqueous solution. Chemosphere 190, 260-266. https://doi.org/10.1016/j.chemosphere.2017.09.140.

Singh, B., Singh, B.P., Cowie, A.L., 2010. Characterisation and evaluation of biochars for their application as a soil amendment. Soil Res. 48 (7), 516-525. https://doi.org/10.1071/SR10058.

Smith, C.R., Hatcher, P.G., Kumar, S., Lee, J.W., 2016. Investigation into the sources of biochar water-soluble organic compounds and their potential toxicity on aquatic microorganisms. ACS Sustain. Chem. Eng. 4 (5), 2550-2558. https://doi.org/10.1021/acssuschemeng.5b01687.

Song, Z., Lian, F., Yu, Z., Zhu, L., Xing, B., Qiu, W., 2014. Synthesis and characterization of a novel MnOx-loaded biochar and its adsorption properties for Cu^{2+} in aqueous solution. Chem. Eng. J. 242, 36-42. https://doi.org/10.1016/j.cej.2013.12.061.

Srivastava, N.K., Majumder, C.B., 2008. Novel biofiltration methods for the treatment of

946 heavy metals from industrial wastewater. J. Hazard. Mater. 151 (1), 1-8.
947 https://doi.org/10.1016/j.jhazmat.2007.09.101.
948 Su, H., Fang, Z., Tsang, P.E., Zheng, L., Cheng, W., Fang, J., Zhao, D., 2016.
949 Remediation of hexavalent chromium contaminated soil by biochar-supported zero-
950 valent iron nanoparticles. J. Hazard. Mater. 318, 533-540.
951 https://doi.org/10.1016/j.jhazmat.2016.07.039.
952 Suliman, W., Harsh, J.B., Abu-Lail, N.I., Fortuna, A., Dallmeyer, I., Garcia-Perez, M.,
953 2016. Influence of feedstock source and pyrolysis temperature on biochar bulk and
954 surface properties. Biomass Bioenergy 84, 37-48.
955 https://doi.org/10.1016/j.biombioe.2015.11.010.
956 Tan, Z., Yuan, S., Hong, M., Zhang, L., Huang, Q., 2020. Mechanism of negative surface
957 charge formation on biochar and its effect on the fixation of soil cd. J. Hazard. Mater.
958 384, 121370. https://doi.org/10.1016/j.jhazmat.2019.121370.
959 Tang, J., Zhu, W., Kookana, R., Katayama, A., 2013. Characteristics of biochar and its
960 application in remediation of contaminated soil. J. Biosci. Bioeng. 116 (6), 653-659.
961 https://doi.org/10.1016/j.jbiosc.2013.05.035.
962 Tepanosyan, G., Sahakyan, L., Belyaeva, O., Asmaryan, S., Saghatelyan, A., 2018.
963 Continuous impact of mining activities on soil heavy metals levels and human health.
964 Sci. Total Environ. 639, 900-909. https://doi.org/10.1016/j.scitotenv.2018.05.211.
965 Tognotti, L., Flytzani-Stephanopoulos, M., Sarofim, A.F., Kopsinis, H., Stoukides, M.,
966 1991. Study of adsorption-desorption of contaminants on single soil particles using
967 the electrodynamic thermogravimetric analyzer. Environ. Sci. Technol. 25 (1), 104-
968 109. https://doi.org/10.1021/es00013a010.
969 Uchimiya, M., 2014. Influence of pH, ionic strength, and multidentate ligand on the

970 interaction of Cd^{II} with biochars. ACS Sustain. Chem. Eng. 2 (8), 2019-2027.
971 https://doi.org/10.1021/sc5002269.
972 Uchimiya, M., Chang, S., Klasson, K.T., 2011. Screening biochars for heavy metal
973 retention in soil: Role of oxygen functional groups. J. Hazard. Mater. 190 (1-3), 432-
974 441. https://doi.org/10.1016/j.jhazmat.2011.03.063.
975 Uchimiya, M., Klasson, K.T., Wartelle, L.H., Lima, I.M., 2011. Influence of soil
976 properties on heavy metal sequestration by biochar amendment: 1. Copper sorption
977 isotherms and the release of cations. Chemosphere 82 (10), 1431-1437.
978 https://doi.org/10.1016/j.chemosphere.2010.11.050.
979 Uchimiya, M., Wartelle, L.H., Klasson, K.T., Fortier, C.A., Lima, I.M., 2011. Influence
980 of pyrolysis temperature on biochar property and function as a heavy metal sorbent
981 in soil. J. Agric. Food. Chem. 59 (6), 2501-2510. https://doi.org/10.1021/jf104206c.
982 Uras, Ü., Carrier, M., Hardie, A.G., Knoetze, J.H., 2012. Physico-chemical
983 characterization of biochars from vacuum pyrolysis of South African agricultural
984 wastes for application as soil amendments. J. Anal. Appl. Pyrolysis 98, 207-213.
985 https://doi.org/10.1016/j.jaap.2012.08.007.
986 Usman, A., Sallam, A., Zhang, M., Vithanage, M., Ahmad, M., Al-Farraj, A., Ok, Y.S.,
987 Abduljabbar, A., Al-Wabel, M., 2016. Sorption process of date palm biochar for
988 aqueous Cd(II) removal: Efficiency and mechanisms. Water Air Soil Pollut. 227 (12).
989 https://doi.org/10.1007/s11270-016-3161-z.
990 Várhegyi, G., Szabó, P., Till, F., Zelei, B., Antal, M.J., Dai, X., 1998. TG, TG-MS, and
991 FTIR characterization of high-yield biomass charcoals. Energy Fuels 12 (5), 969-974.
992 https://doi.org/10.1021/ef9800359.
993 Venderbosch, R.H., Prins, W., 2010. Fast pyrolysis technology development. Biofuel.

994 Bioprod. Bior. 4 (2), 178-208. https://doi.org/10.1002/bbb.205.
995 Wan Ngah, W.S., Hanafiah, M.A.K.M., 2008. Removal of heavy metal ions from
996 wastewater by chemically modified plant wastes as adsorbents: A review. Bioresour.
997 Technol. 99 (10), 3935-3948. https://doi.org/10.1016/j.biortech.2007.06.011.
998 Wang, D., Griffin, D.E., Parikh, S.J., Scow, K.M., 2016. Impact of biochar amendment
999 on soil water soluble carbon in the context of extreme hydrological events.
1000 Chemosphere 160, 287-292. https://doi.org/10.1016/j.chemosphere.2016.06.100.
1001 Wang, G., Li, Y., Wang, G., Cai, K., Xu, Y., 2024. Insights into the photodegradation of
1002 decamethylammonium bromide (DDAB) under UV/H_2O_2 system: Photodegradation
1003 kinetic modeling, degradation mechanism and toxicity evaluation. J. Environ. Chem.
1004 Eng. 12(5):113344. https://doi.org/10.1016/j.jece.2024.113344.
1005 Wang, J., Chen, C., 2009. Biosorbents for heavy metals removal and their future.
1006 Biotechnol. Adv. 27 (2), 195-226. https://doi.org/10.1016/j.biotechadv.2008.11.002.
1007 Wang, L., Li, X., Tsang, D.C.W., Jin, F., Hou, D., 2020. Green remediation of Cd and Hg
1008 contaminated soil using humic acid modified montmorillonite: immobilization
1009 performance under accelerated ageing conditions. J. Hazard. Mater. 387, 122005.
1010 https://doi.org/https://doi.org/10.1016/j.jhazmat.2019.122005.
1011 Wang, M., Zhu, Y., Cheng, L., Andserson, B., Zhao, X., Wang, D., Ding, A., 2018.
1012 Review on utilization of biochar for metal-contaminated soil and sediment
1013 remediation. J. Environ. Sci. 63, 156-173. https://doi.org/10.1016/j.jes.2017.08.004.
1014 Wang, R., Huang, D., Liu, Y., Zhang, C., Lai, C., Zeng, G., Cheng, M., Gong, X., Wan,
1015 J., Luo, H., 2018. Investigating the adsorption behavior and the relative distribution
1016 of Cd^{2+} sorption mechanisms on biochars by different feedstock. Bioresour. Technol.
1017 261, 265-271. https://doi.org/10.1016/j.biortech.2018.04.032.

1018 Wang, Y., Liu, R., 2017. Comparison of characteristics of twenty-one types of biochar
1019 and their ability to remove multi-heavy metals and methylene blue in solution. Fuel
1020 Process. Technol. 160, 55-63. https://doi.org/10.1016/j.fuproc.2017.02.019.
1021 Wang, Z., Liu, G., Zheng, H., Li, F., Ngo, H.H., Guo, W., Liu, C., Chen, L., Xing, B.,
1022 2015. Investigating the mechanisms of biochar's removal of lead from solution.
1023 Bioresour. Technol. 177, 308-317. https://doi.org/10.1016/j.biortech.2014.11.077.
1024 Wasay, S.A., Barrington, S., Tokunaga, S., 2001. Organic acids for the in situ remediation
1025 of soils polluted by heavy metals: Soil flushing in columns. Water Air Soil Pollut.
1026 127 (1), 301-314. https://doi.org/10.1023/A:1005251915165.
1027 Wu, J., Zhou, B., Li, Z., Liu, C., Li, Y., Wang, Y., Zhao, N., Wang, Z., Chai, Y., Scopa,
1028 A., Drosos, M., Rajput, V., Shan, S., 2025. Biochar promoted soil organic carbon
1029 accumulation and aggregate stability by increasing the content of organic complex
1030 metal oxides in paddy soil. Soil Tillage Res. 254, 106713.
1031 https://doi.org/10.1016/j.still.2025.106713.
1032 Wu, P., Cui, P., Fang, G., Wang, Y., Wang, S., Zhou, D., Zhang, W., Wang, Y., 2018.
1033 Biochar decreased the bioavailability of Zn to rice and wheat grains: insights from
1034 microscopic to macroscopic scales. Sci. Total Environ. 621, 160-167.
1035 https://doi.org/10.1016/j.scitotenv.2017.11.236.
1036 Xiao, B., Jia, J., Wang, W., Zhang, B., Ming, H., Ma, S., Kang, Y., Zhao, M., 2023. A
1037 review on magnetic biochar for the removal of heavy metals from contaminated soils:
1038 Preparation, application, and microbial response. J. Hazard. Mater. Adv. 10, 100254.
1039 https://doi.org/10.1016/j.hazadv.2023.100254.
1040 Xiao, Y., Huang, Y., Yu, M., Zhu, Z., Xu, W., Li, Z., Cheng, H., Jin, B., Fei, X., 2025.
1041 Development of silica-modified biochar for sustainable and efficient stabilization of

heavy metals in municipal solid waste incineration fly ash. Waste Manage. 205, 115009. https://doi.org/10.1016/j.wasman.2025.115009.

Xiao, Y., Xue, Y., Gao, F., Mosa, A., 2017. Sorption of heavy metal ions onto crayfish shell biochar: Effect of pyrolysis temperature, pH and ionic strength. J. Taiwan Inst. Chem. Eng. 80, 114-121. https://doi.org/10.1016/j.jtice.2017.08.035.

Xie, T., Sadasivam, B.Y., Reddy, K.R., Wang, C., Spokas, K., 2016. Review of the effects of biochar amendment on soil properties and carbon sequestration. J. Hazard. Toxic. Radio. 20 (1), 4015011-4015013. https://doi.org/10.1061/(ASCE)HZ.2153-5515.0000293.

Xu, M., Wu, J., Luo, L., Yang, G., Zhang, X., Peng, H., Yu, X., Wang, L., 2018. The factors affecting biochar application in restoring heavy metal-polluted soil and its potential applications. Chem. Ecol. 34 (2), 177-197. https://doi.org/10.1080/02757540.2017.1404992.

Xu, R., Zhao, A., 2013. Effect of biochars on adsorption of Cu(II), Pb(II) and Cd(II) by three variable charge soils from southern china. Environ. Sci. Pollut. Res. 20 (12), 8491-8501. https://doi.org/10.1007/s11356-013-1769-8.

Xu, X., Cao, X., Zhao, L., Wang, H., Yu, H., Gao, B., 2013. Removal of Cu, Zn, and Cd from aqueous solutions by the dairy manure-derived biochar. Environ. Sci. Pollut. R. 20, 358-368. https://doi.org/10.1007/s11356-012-0873-5.

Xu, X., Zhao, Y., Sima, J., Zhao, L., Mašek, O., Cao, X., 2017. Indispensable role of biochar-inherent mineral constituents in its environmental applications: A review. Bioresour. Technol. 241, 887-899. https://doi.org/10.1016/j.biortech.2017.06.023.

Xu, Y., Qi, F., Yan, Y., Sun, W., Bai, T., Lu, N., Luo, H., Liu, C., Yuan, B., Sheng, Z., Liu, T., 2023. The interaction of different chlorine-based additives with swine manure

during pyrolysis: Effects on biochar properties and heavy metal volatilization. Waste Manage. 169, 52-61. https://doi.org/10.1016/j.wasman.2023.06.023.

Xu, Z., Xu, X., Tsang, D.C.W., Yang, F., Zhao, L., Qiu, H., Cao, X., 2020. Participation of soil active components in the reduction of Cr(VI) by biochar: Differing effects of iron mineral alone and its combination with organic acid. J. Hazard. Mater. 384, 121455. https://doi.org/10.1016/j.jhazmat.2019.121455.

Yan, C., Li, J., Sun, Z., Wang, X., Xia, S., 2024. Mechanistic insights into removal of pollutants in adsorption and advanced oxidation processes by livestock manure derived biochar: a review. Sep. Purif. Technol. 346, 127457. https://doi.org/10.1016/j.seppur.2024.127457.

Yang, H., Yan, R., Chen, H., Lee, D.H., Zheng, C., 2007. Characteristics of hemicellulose, cellulose and lignin pyrolysis. Fuel 86 (12-13), 1781-1788. https://doi.org/10.1016/j.fuel.2006.12.013.

Yang, X., Huang, C., Sanjeewa, K.K.A., Gao, X., Mao, X., Wang, L., 2025. A comprehensive review of heavy metals in aquatic products and their removal techniques. Food Control 178, 111520. https://doi.org/10.1016/j.foodcont.2025.111520.

Yang, Y., Wei, Z., Zhang, X., Chen, X., Yue, D., Yin, Q., Xiao, L., Yang, L., 2014. Biochar from alternanthera philoxeroides could remove Pb(II) efficiently. Bioresour. Technol. 171, 227-232. https://doi.org/10.1016/j.biortech.2014.08.015.

Ye, L., Gao, G., Li, F., Sun, Y., Yang, S., Qin, Q., Wang, J., Bai, N., Xue, Y., Sun, L., 2025. A comprehensive review on biochar-based materials for the safe utilization and remediation of heavy metal-contaminated agricultural soil and associated mechanisms. J. Environ. Chem. Eng. 13 (3), 116179.

https://doi.org/10.1016/j.jece.2025.116179.

Yin, D., Wang, X., Chen, C., Peng, B., Tan, C., Li, H., 2016. Varying effect of biochar Cd, Pb and As mobility in a multi-metal contaminated paddy soil. Chemosphere 152, 196-206. https://doi.org/10.1016/j.chemosphere.2016.01.044.

Yoon, K., Cho, D., Tsang, D.C.W., Bolan, N., Rinklebe, J., Song, H., 2017. Fabrication of engineered biochar from paper mill sludge and its application into removal of arsenic and cadmium in acidic water. Bioresour. Technol. 246, 69-75. https://doi.org/10.1016/j.biortech.2017.07.020.

Yuan, J., Xu, R., Zhang, H., 2011. The forms of alkalis in the biochar produced from crop residues at different temperatures. Bioresour. Technol. 102 (3), 3488-3497. https://doi.org/10.1016/j.biortech.2010.11.018.

Zhang, C., Shan, B., Tang, W., Zhu, Y., 2017. Comparison of cadmium and lead sorption by *phyllostachys pubescens* biochar produced under a low-oxygen pyrolysis atmosphere. Bioresour. Technol. 238, 352-360. https://doi.org/10.1016/j.biortech.2017.04.051.

Zhang, F., Wang, X., Yin, D., Peng, B., Tan, C., Liu, Y., Tan, X., Wu, S., 2015. Efficiency and mechanisms of Cd removal from aqueous solution by biochar derived from water hyacinth (*eichornia crassipes*). J. Environ. Manage. 153, 68-73. https://doi.org/10.1016/j.jenvman.2015.01.043.

Zhang, T., Zhu, X., Shi, L., Li, J., Li, S., Lü, J., Li, Y., 2017. Efficient removal of lead from solution by celery-derived biochars rich in alkaline minerals. Bioresour. Technol. 235, 185-192. https://doi.org/10.1016/j.biortech.2017.03.109.

Zhang, X., Zhang, P., Yuan, X., Li, Y., Han, L., 2020. Effect of pyrolysis temperature and correlation analysis on the yield and physicochemical properties of crop residue

biochar. Bioresour. Technol. 296, 122318. https://doi.org/10.1016/j.biortech.2019.122318.

Zhang, Z., Zhu, Z., Shen, B., Liu, L., 2019. Insights into biochar and hydrochar production and applications: A review. Energy 171, 581-598. https://doi.org/10.1016/j.energy.2019.01.035.

Zhao, L., Cao, X., Zheng, W., Wang, Q., Yang, F., 2015. Endogenous minerals have influences on surface electrochemistry and ion exchange properties of biochar. Chemosphere 136, 133-139. https://doi.org/10.1016/j.chemosphere.2015.04.053.

Zhao, M., Dai, Y., Zhang, M., Feng, C., Qin, B., Zhang, W., Zhao, N., Li, Y., Ni, Z., Xu, Z., Tsang, D.C.W., Qiu, R., 2020. Mechanisms of Pb and/or Zn adsorption by different biochars: Biochar characteristics, stability, and binding energies. Sci. Total Environ. 717, 136894. https://doi.org/10.1016/j.scitotenv.2020.136894.

Zhao, R., Coles, N., Kong, Z., Wu, J., 2015. Effects of aged and fresh biochars on soil acidity under different incubation conditions. Soil and Till. Res. 146, 133-138. https://doi.org/10.1016/j.still.2014.10.014.

Zhao, S., Zhao, S., Wang, B., 2025. Combined application of biochar and PGPB on crop growth and heavy metals accumulation: A meta-analysis. Environ. Pollut. 381, 126626. https://doi.org/10.1016/j.envpol.2025.126626.

Zhu, N., Yan, T., Qiao, J., Cao, H., 2016. Adsorption of arsenic, phosphorus and chromium by bismuth impregnated biochar: Adsorption mechanism and depleted adsorbent utilization. Chemosphere 164, 32-40. https://doi.org/10.1016/j.chemosphere.2016.08.036.

Zhu, X., Chen, B., Zhu, L., Xing, B., 2017. Effects and mechanisms of biochar-microbe interactions in soil improvement and pollution remediation: A review. Environ. Pollut.

227, 98-115. https://doi.org/10.1016/j.envpol.2017.04.032.

Highlights

- Biochar is widely used to the remediation of heavy metal in water and soil.
- Physicochemical properties and regularity of biochar are elaborated.
- Main factors affecting on the remediation of heavy metal by biochar are explored.
- Differences exist in the mechanisms of heavy metals remediation by biochar.
- The challenges and future studies on the application of biochar are prospected.

Declaration of competing interests

The authors declare that they have no known competing financial interests or personal relationships that could have appeared to influence the work reported in this paper.